Journal of proteome research

pubs.acs.org/jpr

Article

Distinct Proteomic Brain States Underlying Long-Term Memory Formation in Aversive Operant Conditioning

Published as part of Journal of Proteome Research special issue "Canadian Proteomics".

Julia Bandura, Calvin Chan, Hong-Shuo Sun, Aaron R. Wheeler, and Zhong-Ping Feng*

Cite This: *J. Proteome Res.* 2025, 24, 27−45

Read Online

ACCESS | Metrics & More | Article Recommendations | Supporting Information

ABSTRACT: Long-term memory (LTM) formation relies on *de novo* protein synthesis; however, the full complement of proteins crucial to LTM formation remains unknown in any system. Using an aversive operant conditioning model of aerial respiratory behavior in the pond snail mollusk, *Lymnaea stagnalis* (*L. stagnalis*), we conducted a transcriptome-guided proteomic analysis on the central nervous system (CNS) of LTM, no LTM, and control animals. We identified 366 differentially expressed proteins linked to LTM formation, with 88 upregulated and 36 downregulated in LTM compared to both no LTM and controls. Functional annotation highlighted the importance of balancing protein synthesis and degradation for LTM, as indicated by the upregulation of proteins involved in proteasome activity and translation initiation, including EIF2D, mRNA levels of which were confirmed to be upregulated by conditioning and implicated nuclear factor Y as a potential regulator of LTM-related transcription in this model. This study represents the first transcriptome-guided proteomic analysis of LTM formation ability in this model and lays the groundwork for discovering orthologous proteins critical to LTM in mammals.

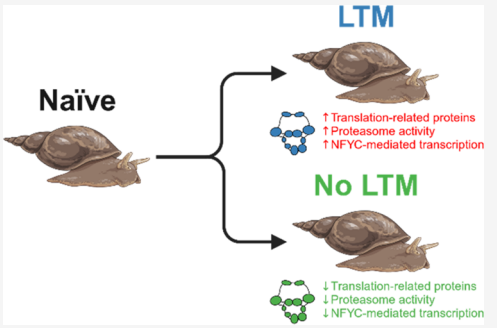

KEYWORDS: *long-term memory, differential proteomics, Lymnaea stagnalis, conditioning, shotgun proteomics, neuroscience*

INTRODUCTION

Long-term memory (LTM) formation relies on *de novo* protein synthesis.[1−4] This process is well known to be driven by learning-dependent regulation of translation initiation.[5,6] However, the identities of newly synthesized proteins, and their signaling pathways and mechanisms as they relate to consolidation and maintenance of LTM, remain unclear. With the advent of high-quality proteomic databases, many studies have attempted to identify the targets of learning-induced novel protein synthesis using both top-down and bottom-up proteomics and bioinformatics approaches in a variety of models. In rodents, proteins regulated by LTM have been identified at various time points and in various relevant brain regions in spatial learning,[7,8] contextual fear conditioning and fear memory,[9−13] auditory learning,[14,15] and oculomotor memory,[16] and include proteins associated with regulation of protein synthesis and degradation,[7,8,11,13,14] metabolism and enzyme activity,[9,12,13] kinase activity,[10,14] cytoskeletal organization,[8,9,14] synaptic function,[16] vesicle-mediated trafficking, and exo/endocytosis.[13−15] Many of these pathways are also regulated in invertebrate models of LTM, such as in *Drosophila melanogaster* visual and olfactory learning models which show differential regulation of synaptic proteins[17] and proteins involved in endocytosis,[18] and proteomic studies of memory-deficient mutants show changes in the abundance of proteins involved in metabolic pathways, protein folding/sorting/degradation, transport proteins, and cell structure regulation.[19] Similar approaches have been applied to mollusks such as *Aplysia californica*[20] and *Hermissenda*[21] to identify differential regulation of proteins involved in metabolism, cytoskeletal regulation, signal transduction, RNA binding, and synaptic function associated with simpler forms of conditioning and memory-associated serotonin-stimulation. Together, these findings suggest that LTM formation is associated with wide-scale changes in protein synthesis in whole brains or brain regions across taxa and that these changes are associated with regulation of a wide variety of protein signaling pathways. However, analyzing differential protein expression by comparing animals subjected to conditioning or training with naïve or sham control ions introduces significant biological ambiguity. It remains unclear which differentially expressed proteins are essential for successful LTM formation following training or learning.

Received: January 25, 2024
Revised: August 20, 2024
Accepted: September 3, 2024
Published: December 10, 2024

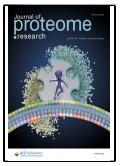

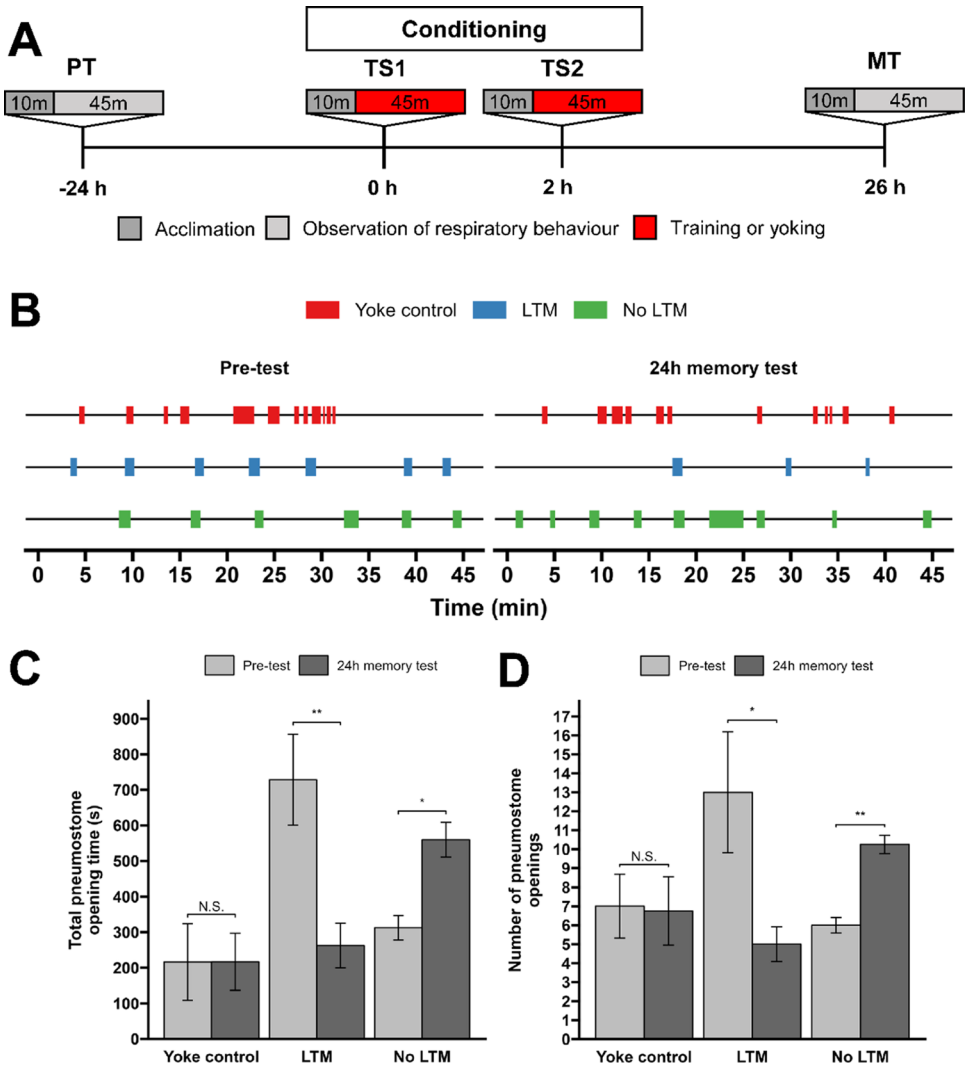

Figure 1. Aversive operant conditioning results in distinct behavioral phenotypes in LTM and no LTM snails. (A) Timeline of behavioral conditioning. 24 h prior to conditioning, basal aerial respiratory behavior is monitored in hypoxia for 45 min during a pretest (PT). Conditioning consists of two training sessions (TS1 and TS2) of 45 min separated by 1 h, during which animals are returned to their home tank. Each training session involves applying a sharp tactile stimulus to the area of the pneumostome each time the animal attempts pneumostome opening. 24 h after the beginning of the second training session, respiratory behavior is once again monitored in hypoxia for 45 min in the memory test (MT). Each observation/training session is preceded by a 10 min acclimation period. Yoke animals undergo an identical procedure but during conditioning receive stimuli agnostic to pneumostome opening state. (B) Example aerial respiratory behavior patterns during the pretest and the 24 h memory test in yoke control, LTM, and no LTM animals. (C) Total pneumostome opening time during pretest (PT) and 24 h memory test (MT) for yoke control, LTM, and no LTM animals. (D) Number of pneumostome openings during pretest (PT) and 24 h memory test (MT) for yoke control, LTM, and no LTM animals. All bar graphs are presented as mean ± standard error of the mean (SEM). Paired *t* test: NS = not significant, $*p < 0.05$, $**p < 0.01$.

To address this, we sought to leverage a molluskan model of LTM formation, aversive operant conditioning of aerial respiratory behavior in the pond snail *Lymnaea stagnalis* (*L. stagnalis*).[22] This form of conditioning, where a sharp tactile stimulus is applied to the animal's pneumostome, or breathing organ, leads to a robust decrease in its respiratory activity and a form of LTM,[22] which can persist up to 4 weeks.[23] Like in other models, LTM following aversive operant conditioning requires protein synthesis.[24,25] Though some proteins both regulated by and crucial to LTM formation have been identified in this model, such as calcium/cAMP-response element-binding protein 1 (CREB1), dynamin-1, syntaxin-1, NMDA receptors, protein kinase C, MAPK, and MEN1,[26−28] large-scale proteomic analyses of LTM-regulated proteins have either relied on bottom-up gel-based approaches[29,30] or have been hampered by a lack of transcriptomic protein-coding sequence data.[31] Most interestingly, we have observed in our previous study that the ability of animals to form LTM is variable in this model, and reported two groups of animals subjected to aversive operant conditioning labeled as capable and incapable of learning based on their ability to form LTM.[32] Therefore, this model presents an advantageous opportunity to examine proteins and signaling pathways regulated not only by training itself but also by successful LTM formation following training, thus identifying pathways that may be crucial to LTM formation.

The quality of the *L. stagnalis* central nervous system (CNS) transcriptome has increased significantly in recent years.[33−35] Recently, our group sequenced the first genome-guided transcriptome of the *L. stagnalis* CNS and generated the

https://doi.org/10.1021/acs.jproteome.4c00055
J. Proteome Res. 2025, 24, 27−45

most comprehensive and well-annotated CNS to date.[36] This presents an unprecedented opportunity to analyze protein sequencing from this model with greater depth and accuracy than ever before. Therefore, in the current study, we sought to identify the proteins and pathways regulated by LTM formation ability following aversive operant conditioning in *L. stagnalis*. We applied a bottom-up shotgun proteomics approach to identify and characterize CNS proteins differentially expressed between LTM, no LTM, and yoke control CNS and identified a set of 366 proteins associated with the ability to form LTM. Functional annotation of these proteins by sequence similarity revealed their involvement in biological processes (BP) such as cellular signaling, cellular organization, metabolic processes, responses to stimuli, and intracellular transport, molecular functions (MFs) such as nucleic acid binding, metabolic activity, protein−protein binding, GTPase binding, and ribosome binding, and cellular compartments such as organelles, cytoskeleton, the proteasome, and the spliceosome. We then identified proteins that appeared to be upregulated or downregulated by LTM and determined, via pathway annotation, that proteins associated with promoting protein synthesis and degradation, such as EIF2D, CPEB2, HERC2, HERC4, PSMC2, and PSMB6 appear to be upregulated by LTM formation ability, as well as the transcription factor NFYC. Finally, we assessed mRNA expression of EIF2D following aversive operant conditioning using reverse transcription-quantitative polymerase chain reaction (RT-qPCR) and demonstrated that EIF2D mRNA is upregulated by conditioning but not in yoke animals. Together, these data identify potential pathways that may be crucial to LTM formation ability following aversive operant conditioning in this model and form the basis for future investigation of the involvement of key translation- and transcription-associated proteins via genetic and pharmacological manipulation.

EXPERIMENTAL PROCEDURES

Animals

Freshwater great pond snails (*L. stagnalis*) were bred and maintained at aquaculture facilities at the University of Toronto, originally obtained from an inbred culture at the Vrije University in Amsterdam, as described previously.[26,27,32,37] The animals were kept in water at 18−25 °C on a 12 h light/12 h dark cycle and were fed lettuce three times a week and fish food flakes once a week. Adult snails of approximately 3.5−4 months of age and having shell length from 20 to 30 mm were used in all experiments. Ethics approval is not required for research work with *L. stagnalis*.

Aversive Operant Conditioning of Aerial Respiratory Behavior

Aversive operant conditioning was conducted as done previously[26,27,32] (Figure 1A). Briefly, in a pretest, pneumostome opening and closing was monitored for 45 min following a 10 min acclimation period, 24 h prior to conditioning, in a 2 L beaker containing 1 L of dechlorinated hypoxic water induced by bubbling with N_2 gas for at least 20 min. Only snails that opened their pneumostomes ≥5 times were conditioned in subsequent experiments. Animals were then returned to their home aquaria.

The next day, animals that qualified for training based on their basal respiratory rates were divided into two groups, one that underwent operant conditioning (trained) and another that underwent yoking (yoke controls). Training or yoking was undertaken as follows: animals acclimated in hypoxic water for 10 min, then either received a sharp tactile stimulus to the area around the pneumostome each time they initiated pneumostome opening[22] (trained) or, in the case of yoke controls, were paired to an animal undergoing training and received a sharp tactile stimulus to the area around the pneumostome each time their paired trained animal received a stimulus, agnostic to whether they made an attempt to open the pneumostome or not (yoked). Stimulus intensity was optimized such that the animal immediately closed the pneumostome but did not initiate the full-body withdrawal response. Training or yoking was conducted in two 45 min sessions separated by an hour. Snails were returned to their home aquaria after training.

24 h after the beginning of the second training session, trained or yoked animals were returned to hypoxic conditions and once again allowed to acclimate for 10 min, after which pneumostome opening and closing was monitored for 45 min during the memory test. Animals were returned to their home aquaria after the memory test. LTM was defined as a memory test (MT) to pretest (PT) total pneumostome opening time ratio of <0.6, while no LTM in trained snails was defined as an MT to PT total pneumostome opening time ratio of >0.8.[32]

Tissue Preparations

Snails were anesthetized with 10% listerine in snail saline (mM: NaCl 51.3, KCl 1.7, $CaCl_2$ 4.1, $MgCl_2$ 1.5, *N*-(2-hydroxyethyl)piperazine-*N*′-ethanesulfonic acid (HEPES) 2, adjusted to pH 7.9 using NaOH) for 5 min and deshelled with curved forceps. Tissue preparations of the isolated central ring ganglia were dissected as described previously[30,33,38] and placed into microcentrifuge tubes prior to flash freezing in liquid nitrogen. Samples were stored at −80 °C until protein extraction.

Sample Preparation

Lysate Preparation. Protein lysates were prepared from four ganglia per group (LTM, no LTM, yoke control) in 100 μL of lysis buffer (20 mM Tris, 150 mM NaCl, 1 mM ethylenediaminetetraacetic acid (EDTA), 1 mM EGTA, 1% NP-40 (v/v), 0.25% sodium deoxycholate (w/v), pH 7.5) containing protease inhibitor cocktail (BioShop Canada, Inc.). Following homogenization using a sonicator and tissue grinding pestle on ice, samples were rocked at 4 °C for 1 h and centrifuged at 13,000 rpm for 15 min, and then the supernatant was transferred to a fresh tube.

Gel-Assisted Sample Preparation for Mass Spectrometry. To remove detergents for mass spectrometry, samples were processed via gel-assisted sample preparation.[39] Briefly, disulfides were reduced with 5 mM tris(2-carboxyethyl)-phosphine (TCEP) then alkylated using 100 mM 2-iodoacetamide (IAA) at 37 °C for 30 min. 30% T acrylamide monomer solution (w/v) was added to the reduced and alkylated protein lysates, vortexed, and mixed with 10% ammonium persulfate (w/v) and tetramethylethylenediamine (TEMED) to form a gel plug, which was diced and washed 6× with 8 mg/mL ammonium bicarbonate in 50/50% acetonitrile (ACN)/water (v/v). The diced gel containing reduced and alkylated protein lysates was then dried by incubating with neat ACN at room temperature until the gel became brittle and white, after which the gel was air-dried at 37 °C for 20 min. 0.01 mg/mL trypsin in 0.5 mM acetic acid and 8 mg/mL ammonium bicarbonate (approximately 1:30 trypsin/protein

https://doi.org/10.1021/acs.jproteome.4c00055
J. Proteome Res. 2025, 24, 27−45

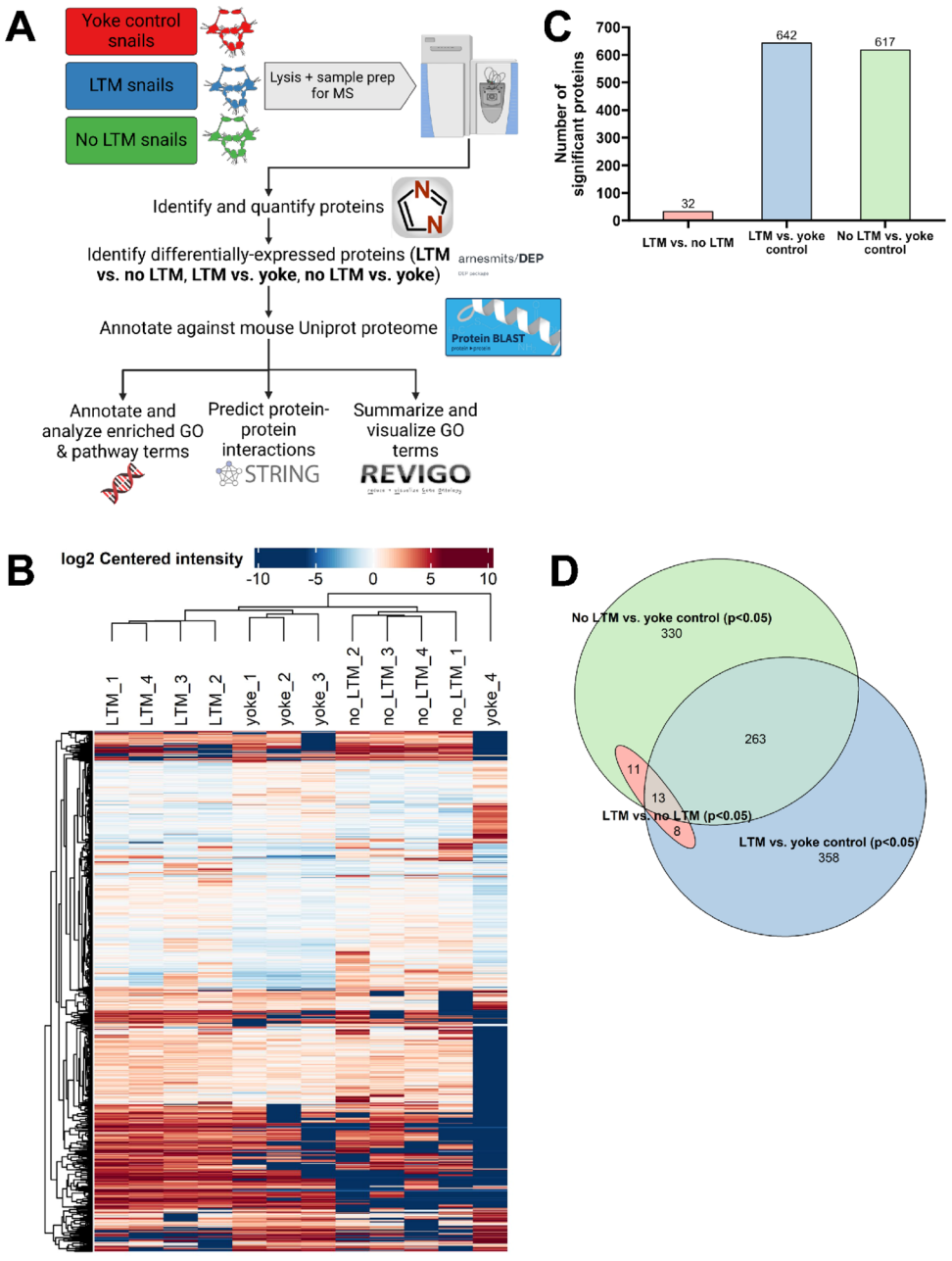

Figure 2. Proteomic identification of LTM-associated proteins. (A) Proteomic identification and functional annotation workflow. Significant differentially expressed proteins lie above the dashed red line, which corresponds to $-\log_{10}(0.05)$. (B) Clustered heatmap of normalized log 2 average MaxLFQ quantification of protein expression in LTM, no LTM, and yoke control CNS samples. (C) Number of significant differentially expressed proteins identified in each comparison ($p < 0.05$). (D) Euler diagram of intersecting significant differentially expressed proteins between each behavioral group. Schematic created in BioRender.

ratio, w/w) was used to digest proteins in-gel overnight at 37 °C. Gel plugs were then extracted with 50:50:0.1% ACN/water/formic acid (v/v/v) by incubating at 37 °C for 15 min six times. The final combined, gel-processed extracts were then vacuum-centrifuged to dryness (SpeedVac, Eppendorf) and reconstituted in aqueous 0.1% formic acid.

Mass Spectrometry

Nanoflow reversed-phase LC was performed on an EASY-nLC 1200 ultrahigh-pressure system coupled to a Q Exactive HF-X mass spectrometer equipped with a nanoelectrospray ion source (Thermo Fisher Scientific). Peptide digests (minimum three technical replicates per sample) were loaded onto a 10 cm fused silica microcapillary column (75 μm i.d., Polymicro Technologies), laser-pulled, and packed in-house with 10 cm of Luna 3 μm C18 100 Å reversed-phase particles (ReproSil-Pur 120 Å, Dr. Maisch GmbH). Mobile phases A and B were water with 0.1% formic acid (v/v) and 80:20:0.1% ACN/water/formic acid (v/v/v), respectively. Peptides were separated at a constant flow rate of 300 nL/min with a linear gradient of 5−30% B within 90 min, followed by a linear increase from 30 to 95% B within 15 min and a 10 min plateau before reequilibration.

Standard shotgun liquid chromatography-mass spectrometry (LC-MS) experiments were performed with a data-dependent top 10 method. A full MS scan range of m/z 350−1400 at a

https://doi.org/10.1021/acs.jproteome.4c00055
J. Proteome Res. 2025, 24, 27−45

resolution of 120,000 at m/z 200 with an AGC target of 3×10^6 ions and maximum injection time of 50 ms was used. Precursor ions with charges of +2 to +6 were isolated with an m/z window of 2 and fragmented by high energy dissociation with a collision energy of 27% at a resolution of 60,000 at m/z 200. MS/MS scans were performed in the Orbitrap with the AGC target, and injection time set to 5×10^5, 250 ms, respectively. Previously targeted precursors were excluded from resequencing for 20 s.

Proteomic Analysis

Raw DDA MS files were analyzed by DIA-NN (version 1.8.1)[40] using a library-free search, based on an *in silico* spectral library generated from predicted protein-coding sequences from the most comprehensive *L. stagnalis* transcriptome to date.[36] All protein-coding sequences are available for BLAST search at https://lymnaea.org and as a fasta file in our MassIVE deposition. Both peptides and proteins were filtered with a maximum false discovery rate (FDR) of 0.01. All unmentioned parameters used the default settings of DIA-NN, and can be found in the file "report_2023oct02.log.txt", which is available in our MassIVE data repository. As DIA-NN is not typically used for protein identification for DDA files, raw DDA MS files were also analyzed in MaxQuant (version 2.4.2.0)[41,42] using the same *L. stagnalis* predicted protein-coding sequences with match-between-runs (MBR) enabled, and filtering of peptides and proteins with a maximum FDR of 0.01. All unmentioned parameters used the default settings of MaxQuant, and can be found in the file "mqpar.xml", which is available in our MassIVE data repository.

Downstream analysis of the DIA-NN output files was performed by R statistical computing environment (version 4.2.2) and the DEP BioConductor package[43] (version DEP_1.20.0). 1% FDR-filtered technical replicates of normalized maximum label-free quantification values (*pg_matrix.tsv file) were averaged for each individual biological replicate, excluding technical replicates for each sample where no protein was detected (NA). The subsequent data set (Supporting Table 1) was used as input to the DEP package, where protein groups that had missing values in all biological replicates of a single experimental group were removed from further analyses. Data were normalized using variance stabilizing transformation using the built-in DEP "normalize_vsn" function. Differential enrichment analysis was conducted using the built-in DEP "test_diff" function, which uses protein-wise linear models and empirical Bayes statistics to test for differentially enriched proteins across all biological replicates. Proteins were considered significantly differentially enriched between experimental groups if the adjusted p-value (FDR q-value) < 0.05 and $\log_2$-fold change > $\log_2(1.5)$. Missing values were imputed as 0 for biological replicates of incomplete groups (i.e., experimental groups with >0 missing values).

Bioinformatics Analysis

As functional annotation information for *L. stagnalis* predicted protein-coding sequences based on transcriptomic data remains limited, identified differentially expressed proteins were functionally annotated by homology using NCBI protein−protein BLAST (version 2.6.0+)[44] against the mouse Uniprot proteome (UP000000589, release 2023_03) using output format 6, max hsps 1, max target seqs 1. Mouse homologues of *L. stagnalis* proteins, taken as the BLASTp hit with the lowest e-value $<1 \times 10^{-5}$, were used for all subsequent functional annotations (Supporting Figure 2). GO terms for each differentially expressed protein were retrieved from the Uniprot knowledgebase[45] and summarized using ReViGO (web server version 1.8.1)[46] into a small (0.5) list. Output plot R scripts were further processed and customized in R using ggplot[47] and output graphs of semantically related terms were visualized using Cytoscape (version 3.10.1).[48] Clustergrammer[49] (web server) was used to visualize clusters of proteins with similar patterns of differential expression between LTM and yoke control, LTM and no LTM, and no LTM and yoke controls. Protein−protein interactions were predicted using STRINGdb[50] using only physical subnetwork prediction and with medium confidence (0.4) and visualized in Cytoscape using the stringApp plugin.[51] Functional enrichment analysis of GO term annotations of proteins associated with LTM and up- and downregulated clusters of LTM-associated proteins was conducted using Enrichr (web server).[52−54] Pathways and terms were considered significantly enriched if enrichment adjusted p-value (FDR) < 0.05 (Figure 2A) against a background consisting of all 3273 proteins observed in the proteomic screen. Finally, sequence alignment was conducted using T-Coffee (web server)[55] and visualized using Jalview.[56] Protein domain analysis was conducted using InterProScan.[57]

RT-qPCR

Total RNA was extracted from whole *L. stagnalis* CNS using the Trizol reagent (Thermo Fisher Scientific) according to the manufacturer's protocols and reverse transcribed into cDNA using Superscript IV Reverse Transcriptase (Thermo Fisher Scientific). Gene-specific primers were designed based on transcript sequences using PrimerQuest (Integrated DNA Technologies) with the following sequences: *Eif2d* (evgLocus_scallop_AF_8451; forward: 5′-AAAGAGTCTGGGATAGCCAAAG-3′, reverse: 5′-TGGGATTAGCTTGTTGGAGATT-3′) and *β-actin* (evgLocus_Scallop_DRR_20351; forward: 5′-TATCCACGAGACCACCTACAA-3′, reverse: 5′-CAGCAATGCCTGGGTACATA-3′). Data were analyzed using the ΔC_t method and normalized to the reference gene, *β-actin*.

RESULTS

Animals Have Variable Learning Performance Following Aversive Operant Conditioning of Aerial Respiratory Behavior

Aversive operant conditioning was performed as done previously in our laboratory[26,27,32] (Figure 1A). Animals' respiratory behavior was observed 24 h prior to and 24 h after conditioning, where timings of pneumostome opening and closing were noted and observed to decrease in frequency and duration of opening in LTM but not in no LTM or yoke control animals (Figure 1B). Total pneumostome opening time decreased significantly in the LTM (728.75 ± 127.68 in PT vs 262.50 ± 62.54 in MT; paired t test $p = 0.00642$) but not the yoke (216.50 ± 107.69 in PT vs 216.75 ± 80.03 in MT; paired t test $p = 0.9959$) or no LTM (312.50 ± 34.06 in PT vs 560.00 ± 48.94 in MT; paired t test $p = 0.02026$) animals following training/yoking (Figure 1C). Similarly, the number of pneumostome openings decreased significantly from the pretest in the LTM (13.00 ± 3.19 in PT vs 5.00 ± 0.91 in MT; paired t test $p = 0.04052$) but not yoke (7.00 ± 1.68 in PT vs 6.75 ± 1.80 in MT; paired t test $p = 0.7177$) or no LTM (6.00 ± 0.41 in PT vs 10.25 ± 0.48 in MT; paired t test $p = 0.006627$) animals 24 h following conditioning (Figure 1D).

https://doi.org/10.1021/acs.jproteome.4c00055
J. Proteome Res. 2025, 24, 27−45

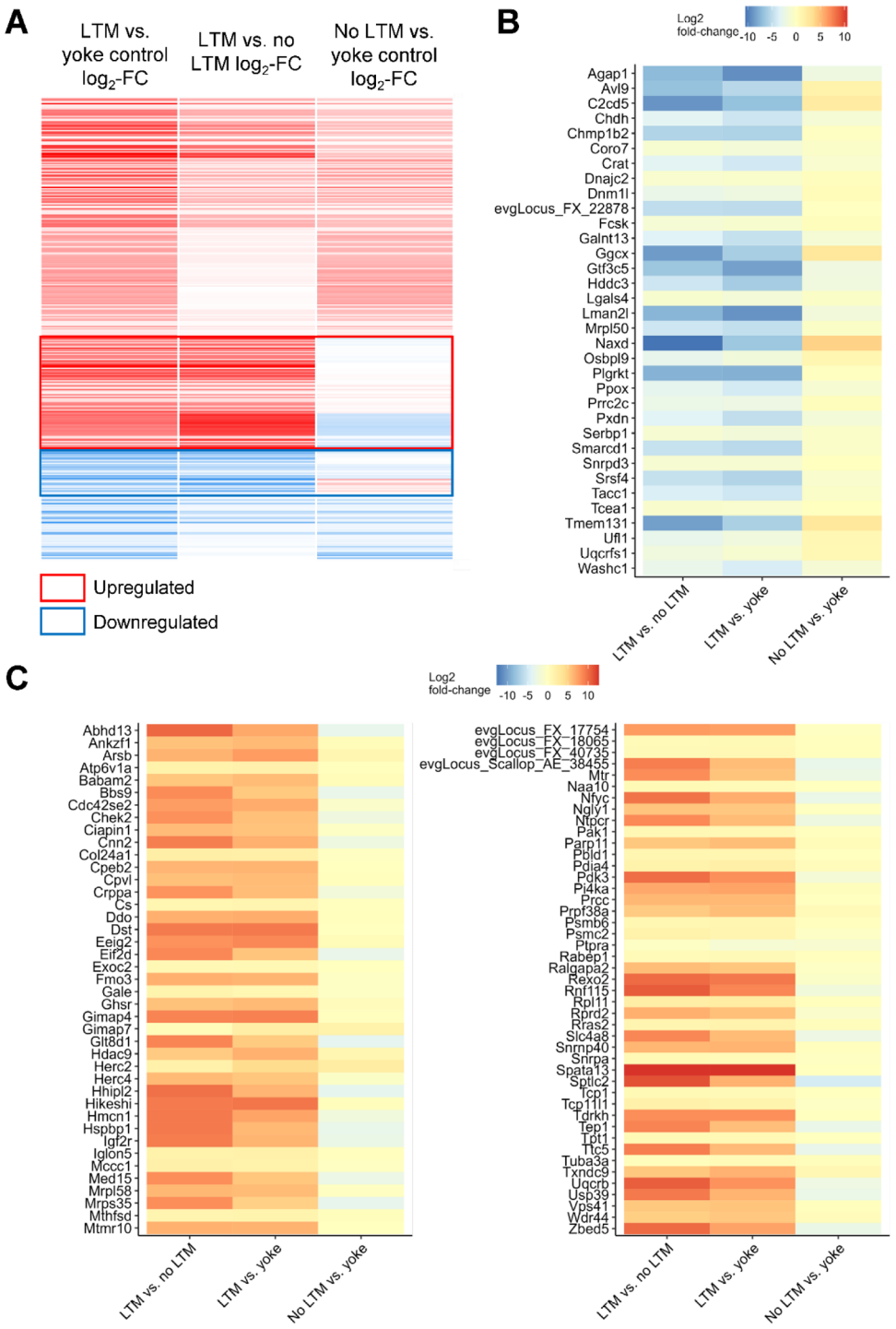

Figure 3. Clustergrammer clustering of proteins based on log_2-fold change between groups identifies proteins up- and downregulated and associated with LTM formation. (A) Using Clustergrammer,[49] LTM-associated proteins were scaled row-wise and hierarchically clustered based on log_2-fold change in expression between LTM and yoke control, LTM and no LTM, and no LTM and yoke control CNS. Two sets of regulated proteins were identified. The "upregulated" set was identified as the set of proteins that had strongly positive (dark red) normalized LTM vs no LTM and LTM vs yoke control log_2-fold changes while normalized no LTM vs yoke control remained weakly positive, close to zero, or negative (blue) (outlined in red). Conversely, the "downregulated" set was identified as the set of proteins that had strongly negative (dark blue) normalized LTM vs no LTM and LTM vs yoke control log_2-fold changes while normalized no LTM vs yoke control remained weakly negative, close to zero, or positive (outlined in blue). (B) Gene symbols and raw log_2-fold change values for proteins identified as downregulated in LTM. (C) Gene symbols and raw log_2-fold change values for proteins identified as upregulated in LTM.

Mass Spectrometric Analysis of *L. stagnalis* CNS Proteins Establishes the Proteomic Trace of LTM Formation Ability

In order to identify the set of proteins associated with LTM formation ability, we established an analysis pipeline for the identification and characterization of CNS proteins from LTM, no LTM, and yoke animals. Immediately following the 24 h memory test, the whole CNS of yoke control (n = 4), LTM (n = 4), and no LTM (n = 4) animals were dissected and lysed in

https://doi.org/10.1021/acs.jproteome.4c00055
J. Proteome Res. 2025, 24, 27−45

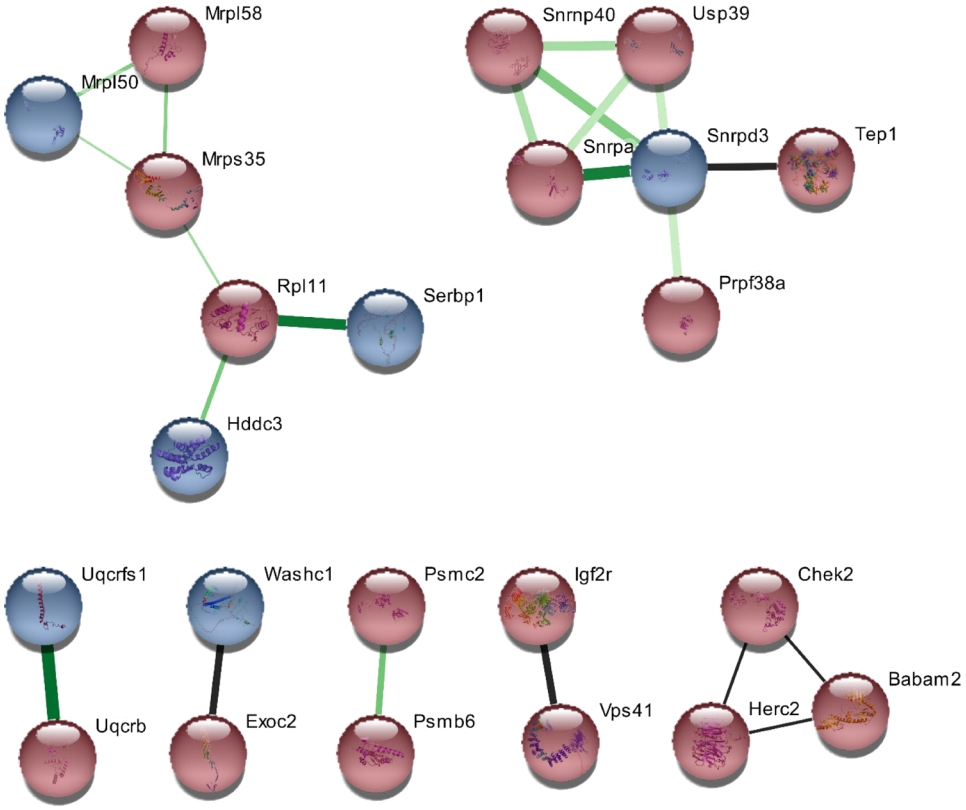

Figure 4. STRING protein−protein interaction prediction identifies clusters of interacting proteins within up- and downregulated LTM-associated proteins. Proteins identified as upregulated or downregulated within the set of LTM-associated proteins were annotated against the STRING database (PPI enrichment *p*-value = 0.00815).[50] Those proteins that were part of a physical subnetwork (i.e., where evidence of interaction was found in textmining, experimental evidence, and protein−protein interaction databases) and with a confidence level of >0.4 are shown, where interactions with experimental evidence have green lines (darker green indicates higher experimental evidence score) and interactions with only textmining or database evidence have black lines. For all lines, the width indicates the STRING score for the interaction, with wider lines corresponding to higher STRING interaction confidence. Labels correspond to gene symbols of associated proteins.

preparation for LC-MS/MS. Following mass spectrometry, DIA-NN[40] was used for protein identification from peptides based on protein sequences predicted from protein-coding transcripts in our high-throughput *L. stagnalis* transcriptome[36] to take advantage of the increased power of neural networks for the library generation of the predicted proteome, thus improving accurate identification. Compared to a MaxQuant library search using the same predicted *L. stagnalis* proteome, DIA-NN analysis identified 3273 *L. stagnalis* proteins compared to MaxQuant analysis, which identified 1030 (Supporting Figure 1A). Additionally, 94% (969) of proteins identified by MaxQuant were also identified by DIA-NN, demonstrating the superiority of DIA-NN analysis for the identification of proteins in our samples (Supporting Figure 1B). Though an *L. stagnalis* proteome has been published using a similar approach,[58] we chose to utilize our published reference transcriptome to create a translated proteome due to a larger number of protein-coding transcripts identified. To infer function by sequence similarity, we annotated identified proteins against the UniProt *Mus musculus* proteins via protein−protein BLAST. The top *M. musculus* protein−protein BLAST hit with *e*-value $<1 \times 10^{-5}$ (Supporting Figure 2) for each identified *L. stagnalis* protein was subsequently used for functional annotation via GO term enrichment, pathway enrichment, and STRING interactor prediction analysis (Figure 2A). Differentially expressed proteins based on label-free quantification (LFQ) values were identified by using the DEP package for R (Supporting Table 2) in order to identify differentially expressed proteins between LTM and no LTM (Supporting Figure 3A), LTM and yoke control (Supporting Figure 3B), and no LTM and yoke control (Supporting Figure 3C) CNS. In total, 3274 predicted *L. stagnalis* proteins were identified (Figure 2B). Of these, 32 were significantly differentially expressed in LTM vs no LTM, 642 were significantly differentially expressed in LTM vs yoke control, and 617 were significantly differentially expressed in no LTM vs yoke control (Figure 2C).

In order to identify proteins uniquely associated with LTM formation ability, we then identified the intersections and differences between the three significantly differentially expressed protein sets. Significant proteins uniquely differentially expressed between LTM and yoke control CNS as well as differentially expressed proteins common to both the LTM vs yoke control and LTM vs no LTM sets were considered to be associated with the ability to form LTM (Figure 2D). In total, we identified 366 proteins associated with the ability to form LTM (Supporting Table 3) that were used for subsequent bioinformatic analyses.

GO Term Annotation Reveals LTM-Associated Protein Functions

To determine the potential functions of LTM-associated proteins, we retrieved GO terms associated with the 366 proteins from the UniProt Knowledgebase[45] and performed semantic multidimensional scaling of related GO terms using

https://doi.org/10.1021/acs.jproteome.4c00055
J. Proteome Res. 2025, 24, 27−45

Table 1. Top 10 Reactome Pathways for Each Up- and Downregulated LTM-Associated Protein Set

reactome pathway	expression pattern	*p*-value	adjusted *p*-value (FDR)	associated genes
G2/M checkpoints R-HSA-69481	↑	2.41×10^{-05}	0.00849	PSMB6; BABAM2; HERC2; CHEK2; PSMC2; REXO2
G2/M DNA damage checkpoint R-HSA-69473	↑	2.30×10^{-04}	0.0297	BABAM2; HERC2; CHEK2; REXO2
metabolism R-HSA-1430728	↑	2.53×10^{-04}	0.0297	MTMR10; UQCRB; NFYC; MCCC1; RPL11; MTR; FMO3; MED15; DDO; PSMB6; CS; GALE; SPTLC2; CHEK2; PSMC2; PI4KA; PDK3; CIAPIN1; ARSB
cell cycle checkpoints R-HSA-69620	↑	6.53×10^{-04}	0.0398	PSMB6; BABAM2; HERC2; CHEK2; PSMC2; REXO2
mRNA splicing—major pathway R-HSA-72163	↑	6.99×10^{-04}	0.0398	SNRNP40; PRPF38A; PRCC; USP39; SNRPA
mRNA splicing R-HSA-72172	↑	8.50×10^{-04}	0.0398	SNRNP40; PRPF38A; PRCC; USP39; SNRPA
Cargo trafficking to periciliary membrane R-HSA-5620920	↑	9.69×10^{-04}	0.0398	TCP1; BBS9; EXOC2
translocation of SLC2A4 (GLUT4) to plasma membrane R-HSA-1445148	↑	0.00103	0.0398	RALGAPA2; REXO2; EXOC2
ubiquitin-mediated degradation of phosphorylated Cdc25A R-HSA-69601	↑	0.00103	0.0398	PSMB6; CHEK2; PSMC2
Chk1/Chk2 (Cds1) mediated inactivation of cyclin B:Cdk1 complex R-HSA-75035	↑	0.00113	0.0398	CHEK2; REXO2
RNA polymerase II transcription termination R-HSA-73856	↓	0.00485	0.187	SRSF4; SNRPD3
choline catabolism R-HSA-6798163	↓	0.00929	0.187	CHDH
GDP-fucose biosynthesis R-HSA-6787639	↓	0.00929	0.187	FCSK
regulation of cytoskeletal remodeling and cell spreading by IPP complex components R-HSA-446388	↓	0.0124	0.187	PXDN
defective factor IX causes hemophilia B R-HSA-9668250	↓	0.0124	0.187	GGCX
β-oxidation of pristanoyl-CoA R-HSA-389887	↓	0.0139	0.187	CRAT
cross-linking of collagen fibrils R-HSA-2243919	↓	0.0154	0.187	PXDN
γ-carboxylation of protein precursors R-HSA-159740	↓	0.0154	0.187	GGCX
SLBP independent processing of histone pre-mRNAs R-HSA-111367	↓	0.0154	0.187	SNRPD3
γ-carboxylation, transport, and amino-terminal cleavage of proteins R-HSA-159854	↓	0.0170	0.187	GGCX

ReViGO.[46] Biological process (BP) GO terms occurring within the LTM formation-associated protein set formed clusters of related terms, including those involved in regulatory processes (Supporting Figure 4A), cellular organization (Supporting Figure 4B), metabolic processes (Supporting Figure 4C), cellular responses to molecules (Supporting Figure 4D), and intracellular transport (Supporting Figure 4E). LTM-associated molecular function (MF) GO terms formed clusters of terms associated with metabolic activity (Supporting Figure 5A), nucleic acid binding and translation (Supporting Figure 5B), protein−protein binding (Supporting Figure 5C), ATPase/GTPase binding (Supporting Figure 5D), and ribosome binding (Supporting Figure 5E). Finally, LTM-associated cellular component (CC) GO terms formed a large cluster of cytosolic terms, including those associated with vesicles, organelles, cytoskeleton, proteasome, and spliceosome (Supporting Figure 6).

Clusters of Similarly Regulated Proteins Identify Potential Protein Signaling Pathways Upregulated and Downregulated by LTM

In order to identify proteins with similar expression patterns between our three conditions, we used Clustergrammer[49] to cluster proteins associated with the ability to form LTM based on their LTM vs no LTM, LTM vs yoke control, and no LTM vs yoke control row-wise scaled $\log_2$-fold expression change values. The interactive Clustergrammer heatmap can be found at the following link: https://maayanlab.cloud/clustergrammer/viz/657f8a7da2b01c00101eeac2/set1_clustergrammer.txt. We determined proteins to be "upregulated in LTM" if their $\log_2$-fold changes for LTM vs no LTM and LTM vs yoke control were strongly positive while their $\log_2$-fold change for no LTM vs yoke control was close to zero or negative. Conversely, we determined proteins to be "downregulated in LTM" if their scaled $\log_2$-fold changes for LTM vs no LTM and LTM vs yoke control were strongly negative while their $\log_2$-fold change for no LTM vs yoke control was close to zero or positive. We thus identified 88 proteins as upregulated in LTM and 36 proteins as downregulated in LTM, which were used in subsequent bioinformatic analyses (Figure 3A). The gene symbols of downregulated in LTM proteins and their raw $\log_2$-fold change values are shown in Figure 3B, while the gene symbols of upregulated in LTM proteins and their raw $\log_2$-fold change values are shown in Figure 3C. Note that while the Clustergrammer heatmap is scaled row-wise, heatmaps in Figure 3B,C represent raw $\log_2$-fold change values, thus colors differ slightly while relative $\log_2$-fold change patterns remain similar.

Proteins Regulated by LTM Formation Form Physical Interaction Networks

To determine potential interaction clusters of proteins differentially regulated by LTM, we predicted physical protein−protein interactions between proteins upregulated and downregulated by LTM using STRINGdb.[50] Indeed, several predicted physical interaction complexes were found to be regulated by LTM formation (Figure 4). For instance,

https://doi.org/10.1021/acs.jproteome.4c00055
J. Proteome Res. 2025, 24, 27−45

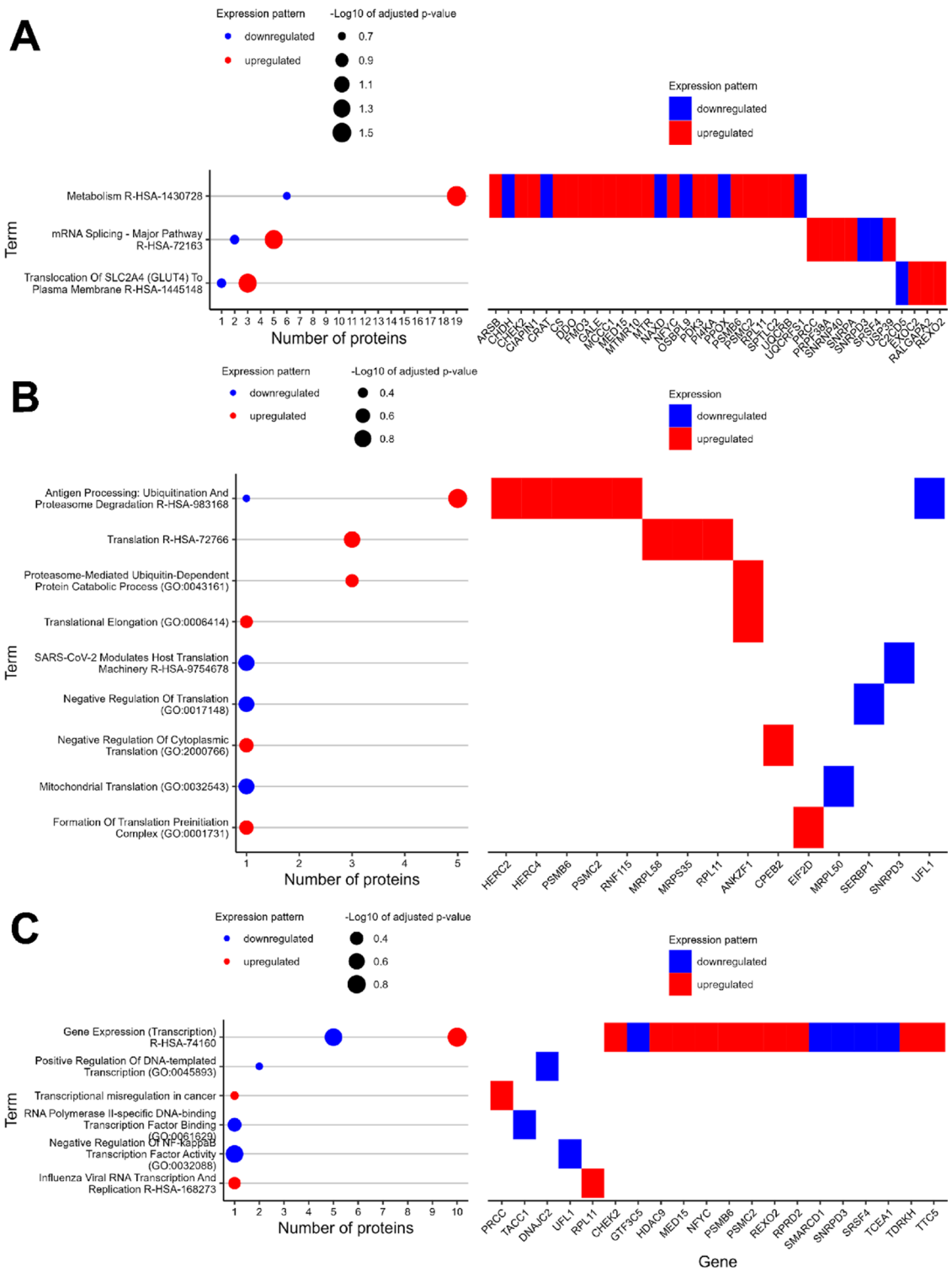

Figure 5. Identities and relative expression pattern of proteins associated with LTM formation as related to common and relevant pathway and GO terms. (A) Terms enriched in upregulated protein set with hits to downregulated proteins, along with identities of proteins corresponding to these terms. (B) Protein synthesis- and protein degradation-related terms in upregulated and downregulated protein sets, along with identities of proteins corresponding to these terms. (C) Transcription-related terms in upregulated and downregulated protein sets along with identities of proteins corresponding to these terms. For all term plots, larger dot sizes indicate higher $-\log_{10}$ adjusted *p*-values, while red and blue indicate that terms are associated with upregulated and downregulated protein sets, respectively. For all protein plots, filled rectangles and their color indicate the presence and regulation of a protein for a particular term, with red corresponding to upregulated and blue corresponding to downregulated. In cases where proteins correspond to multiple pathway or GO terms, the protein is shown as a member of the largest, and therefore most common, term to which it belonged.

upregulated proteins large ribosomal subunit protein uL5 (Rpl11), small ribosomal subunit protein bS1m (Mrps35), and large ribosomal subunit protein mL62 (Mrpl58) were found to form an interaction complex with the downregulated proteins

https://doi.org/10.1021/acs.jproteome.4c00055
J. Proteome Res. 2025, 24, 27−45

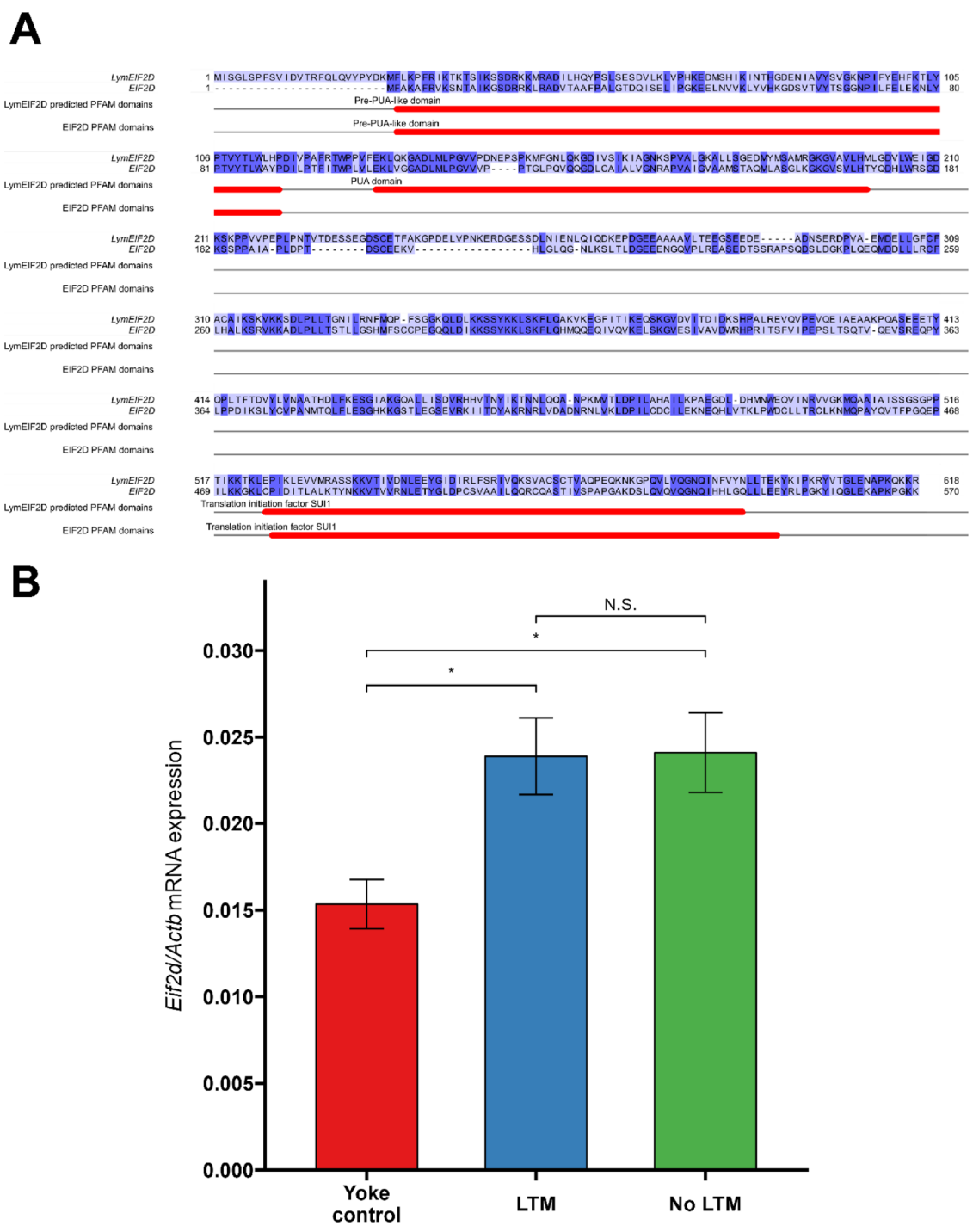

Figure 6. Proposed LymEIF2D mRNA expression is upregulated in aversive operant conditioning. (A) Sequence alignment of the protein sequence of LymEIF2D with its closest mouse homologue, EIF2D (Q61211). (B) mRNA expression of *LymEif2d* relative to reference gene *LymActb* in yoke control ($n = 4$), LTM ($n = 4$), and no LTM ($n = 4$) CNS. Bar graph is presented as mean ± SEM. Unpaired t test with Bonferroni correction: NS = not significant, $^*p < 0.05$.

SERPINE1 mRNA-binding protein 1 (Serbp1), mitochondrial ribosomal protein L50 (Mrpl50), and HD domain containing 3 (Hddc3), suggesting that regulation of mitochondrial proteins and their interactors is associated with LTM formation. Additionally, the presence of a predicted protein complex consisting of upregulated proteins U5 small nuclear ribonucleoprotein 40 kDa protein (Snrnp40), U1 small nuclear ribonucleoprotein A (Snrpa), ubiquitin carboxyl-terminal hydrolase 39 (Usp39), telomerase-associated protein 1 (Tep1), PRP38 pre-mRNA processing factor 38 (yeast) domain containing A (Prpf38a), and downregulated protein small nuclear ribonucleoprotein Sm D3 (Snrpd3) suggests that differential regulation of mRNA splicing may be associated with LTM formation. Meanwhile, the predicted protein complexes consisting of: serine/threonine-protein kinase Chk2 (Chek2), BRISC and BRCA1-A complex member 2 (Babam2), and E3 ubiquitin protein ligase HERC2 (Herc2); vacuolar protein sorting-associated protein 41 homologue

https://doi.org/10.1021/acs.jproteome.4c00055
J. Proteome Res. 2025, 24, 27−45

(Vps41) and cation-independent mannose-6-phosphate receptor (Igf2r); and proteasome subunit β type-6 (Psmb6) and 26S proteasome regulatory subunit 7 (Psmc2) were upregulated in LTM, suggesting that the protein degradation and transport functions of these proteins may be upregulated in LTM. Finally, ubiquinol-cytochrome *c* reductase binding protein (Uqcrb) was found to be upregulated and predicted to bind the downregulated ubiquinol-cytochrome *c* reductase, Rieske iron−sulfur polypeptide 1 (Uqcrfs1), and the upregulated exocyst complex component 2 (Exoc2) was predicted to bind the downregulated WASH complex subunit 1 (Washc1), suggesting that LTM formation may involve differential action of pathways involving these proteins.

Proteins Regulated by LTM Formation Are Involved in the Regulation of Protein Turnover and Transcription

LTM formation following aversive operant conditioning is associated with the expression of proteins involved in mRNA splicing, transcription, and protein synthesis and degradation balance. Following Clustergrammer identification of up- and downregulated proteins associated with LTM formation, we performed Enrichr[52−54] GO and pathway enrichment analysis of each set of proteins to identify potential pathways up- and downregulated in LTM. The top 10 Reactome pathways by *p*-value for the up- and downregulated protein sets are shown in Table 1.

Several pathways were found to be significantly enriched in the upregulated LTM-associated protein sets, which despite being nonsignificantly enriched in the downregulated LTM-associated protein sets also had several hits to downregulated proteins and included metabolism, mRNA splicing, and translocation of SLC2A4 (GLUT4) to the plasma membrane, suggesting that different protein components of these pathways may be differentially regulated in LTM. For instance, mRNA splicing proteins PRCC, USP39, SNRPA, SNRNP40, and PRPF38A are upregulated in LTM, while mRNA splicing proteins SNRPD3 and SRSF4 are downregulated in LTM (Figure 5A).

As changes in protein synthesis[2,6,59] and degradation[60] are well known to be involved in LTM, we investigated whether translation and proteasome GO and pathway terms and associated proteins were associated with proteins regulated in LTM. Indeed, while pathways associated with proteasome activity and translation were not significantly enriched relative to the experimental background in the protein set up- and downregulated by LTM, a number of proteins with annotated terms and pathways corresponding to protein synthesis and degradation were present in our upregulated protein set, such as ubiquitination/proteasome degradation proteins HERC2, HERC4, PSMB6, PSMC2, RNF115, and ANKZF1 and the translational proteins MRPL58, MRPS35, and RPL11, as well as more specific regulators of cytoplasmic translation such as CPEB2 and EIF2D. Interestingly, protein synthesis and degradation pathway term-associated proteins also included several from the downregulated LTM set, including UFL1, which mapped to ubiquitination/proteasome degradation, as well as regulators of translation MRPL50, SERBP1, and SNRPD3 (Figure 5B). Finally, as transcription is well known to be regulated by and critical to LTM formation,[61−66] we investigated whether transcription-related terms were associated with proteins present in our regulated in LTM sets. As expected, the majority of transcription-related annotations were associated with the upregulated in the LTM set of proteins, though several downregulated in LTM proteins also mapped to transcription-related terms, such as "Positive Regulation of DNA-Templated Transcription" (GO:0045893), "RNA Polymerase II-specific DNA-binding Transcription Factor Binding" (GO:0061629), and "Negative Regulation of NF-kappaB Transcription Factor Activity" (GO:0032088). Upregulated proteins involved in transcription include PRCC, RPL11, CHEK2, HDAC9, MED15, NFYC, PSMB6, PSMC2, REXO2, RPRD2, TDRKH, and TTC5. Meanwhile, downregulated proteins involved in transcription included TACC1, DNAJC2, UFL1, GTF3C5, SMARCD1, SNRPD3, SRSF4, and TCEA1 (Figure 5C). Together, these data imply a key role of metabolism, mRNA splicing, and GLUT4 transport pathway activation in LTM, and suggest that expression of proteins involved in protein synthesis, protein degradation, and transcription, while generally upregulated, may involve targeted suppression of the expression of proteins involved in specific subprocesses of these critical LTM-related functions.

LymEIF2D mRNA Expression is Upregulated by Aversive Operant Conditioning

Having identified a number of proteins differentially expressed in LTM formation, we performed a set of RT-qPCR experiments to validate whether mRNA expression of an identified protein of interest, EIF2D, was correlated to its protein levels as quantified in our mass spectrometry experiments. Mass spectrometry results showed that LymEIF2D was significantly increased in LTM vs yoke control CNS (adjusted *p*-value = 0.0227), increased, while not significantly, in LTM vs no LTM CNS (adjusted *p*-value = 0.0992), and decreased, though not significantly, in no LTM vs yoke (adjusted *p*-value = 0.1391) (Supporting Table 2). The proposed *L. stagnalis* EIF2D predicted protein-coding sequence shares 41.391% identity with its top mouse protein−protein BLAST hit (*e*-value = 7.09×10^{-131}), eIF2D (UniProt accession Q61211) (Supporting Table 1; Figure 6A). Therefore, in the absence of an appropriate antibody, we tested whether mRNA levels of LymEIF2D were altered by LTM formation in a new set of LTM ($n = 4$), no LTM ($n = 4$), and yoke control ($n = 4$) CNS samples immediately following the memory test. Indeed, LymEIF2D mRNA expression was significantly increased in LTM compared to yoke controls (0.0239 ± 0.00222 vs 0.0153 ± 0.00142; unpaired *t* test with Bonferroni correction *p*-value = 0.045) (Figure 6B), validating that the protein levels of our proteomic results are correlated with changes in mRNA expression in LTM and yoke control animals. However, LymEIF2D mRNA expression was also significantly increased in no LTM CNS vs yoke controls (0.0241 ± 0.00230 vs 0.0153 ± 0.00142; unpaired *t* test with Bonferroni correction *p*-value = 0.04), suggesting that while aversive operant conditioning may upregulate LymEIF2D mRNA levels, these transcripts may not be translated or may be selectively degraded following translation selectively in no LTM animals.

DISCUSSION

In this study, we identified and characterized differentially expressed CNS proteins associated with LTM formation using a combined behavioral, proteomic, and bioinformatics approach. We have identified several protein signaling pathways for further investigation into their specific roles in LTM formation and consolidation, including the regulation of

https://doi.org/10.1021/acs.jproteome.4c00055
J. Proteome Res. 2025, 24, 27−45

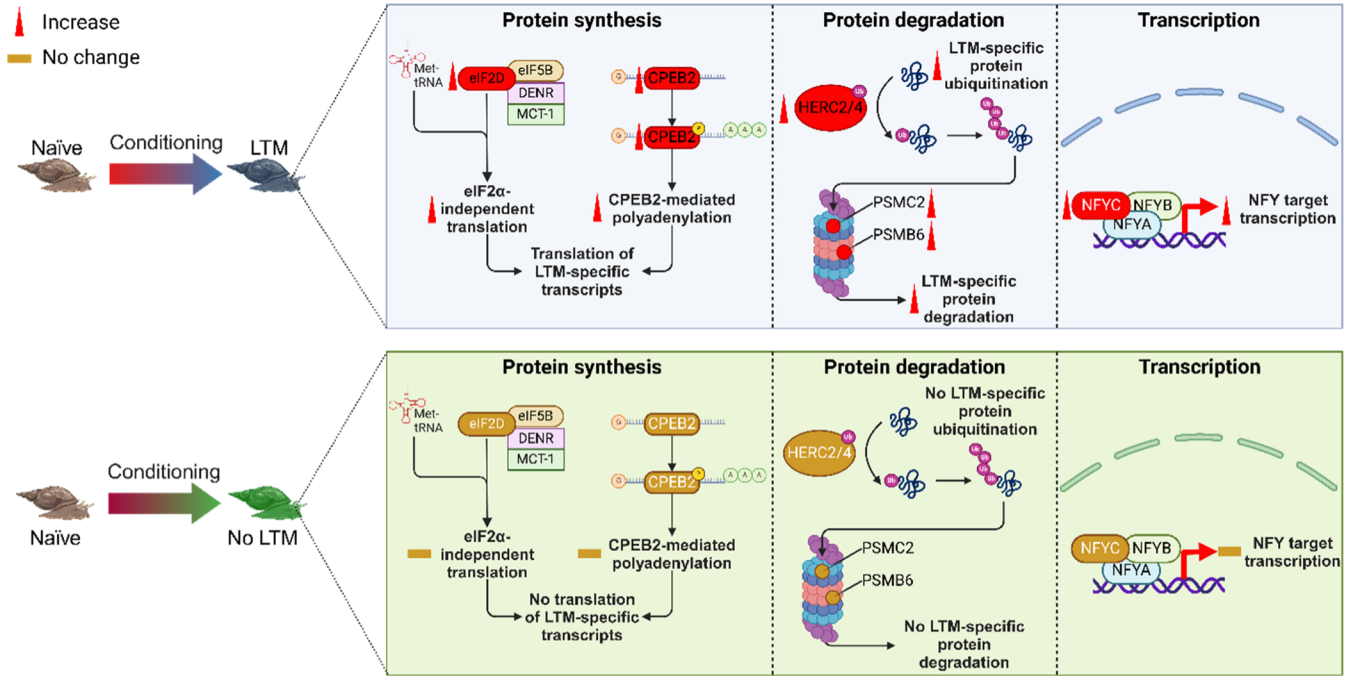

Figure 7. Protein signaling pathways associated with the LTM formation ability following aversive operant conditioning. LTM formation following aversive operant conditioning in *L. stagnalis* is associated with increased expression of eIF2D and CPEB2, which may promote translation of as yet unknown LTM-specific transcripts via eIF2α-independent and polyadenylation-dependent translation, respectively, specifically in LTM but not in no LTM animals. Increases in HERC2 and HERC4, E3 ubiquitin ligases, may promote ubiquitination of LTM-specific transcripts, which may then be targeted for degradation by upregulated PSMC2 and PSMB6, components of the proteasome complex, leading to LTM-specific protein degradation, specifically in LTM but not no LTM animals. Finally, increased NFYC activation in LTM but not no LTM animals following aversive operant conditioning may lead to increased transcription of NFY transcription targets. Schematic created in BioRender.

protein synthesis, protein degradation, and transcription. Finally, we have confirmed that a proposed *L. stagnalis* translation initiation factor, LymEIF2D, is upregulated at least on the mRNA level following aversive operant conditioning, validating the results of our mass spectrometry experiments.

Functions of Differentially Expressed Proteins Associated with LTM Formation

We identified significant proteins uniquely differentially expressed between LTM and yoke control and between LTM and no LTM CNS and identified the potential functions of these proteins. Several *L. stagnalis* proteins to be involved in translation regulation were identified as upregulated in LTM according to our criteria, such as the proposed *Lymnaea* homologues of eukaryotic translation initiation factor 2D (EIF2D), cytoplasmic polyadenylation element-binding protein 2 (CPEB2), HECT and RLD domain containing E3 ubiquitin protein ligase 2 and 4 (HERC2/4), proteasome 26S subunit, ATPase 2 (PSMC2), proteasome 20S subunit β 6 (PSMB6), and nuclear transcription factor Y subunit γ (NFYC) (Figure 7). We further validated the observed increase in the expression of LymEIF2D on the mRNA level following aversive operant conditioning, confirming that this protein may be involved in LTM formation in this model.

Protein Synthesis and Degradation. Alterations in protein synthesis are well known to be associated with LTM formation, and accordingly, several proteomic LTM screens have identified translation-related proteins as differentially expressed and associated with learning.[8,13,19,67] While LTM-associated translation initiation of *de novo* protein synthesis is canonically regulated by eukaryotic translation initiation factor eIF2α,[5,68−70] eIF2D (previously erroneously named ligatin[71]), which we identified as upregulated by LTM on the protein level and upregulated by aversive operant conditioning on the mRNA level, is implicated in noncanonical translation initiation events, such as reinitiation[72] and non-AUG translation initiation,[73−75] particularly in promotion of translation of ATF4,[76] suggesting that its action may counteract LTM-associated eIF2α phosphorylation-mediated repression of ATF4 translation.[68] ATF4, in turn, represses CREB and therefore LTM,[77,78] including in another model of *L. stagnalis* associative learning.[79] While the role of ATF4 has not been established in the current model of LTM formation, as CREB1 expression has also been shown to be essential to LTM following aversive operant conditioning,[27] ATF4 may play a similar role. It would therefore be of interest to compare ATF4 activity between CNS of LTM and no LTM animals in this model, as increased eIF2D expression in LTM vs no LTM animals would suggest increased ATF4 translation, though this effect may be balanced by a conserved decrease in phosphorylated eIF2α. Upregulation of eIF2D associated with LTM formation and conditioning also suggests that transcripts selectively translated via reinitiation events via DENR-MCT-1, such as those related to cell proliferation and signaling,[72] may be regulated by LTM formation in this model. It may therefore be of interest to specifically profile translation of DENR-dependent, eIF2α-independent transcripts in LTM vs no LTM animals to determine whether this process may represent a novel mechanism for protein synthesis that may be critical to LTM formation in this model.

We identified cytoplasmic polyadenylation element-binding protein 2 (CPEB2) as upregulated in LTM in our proteomic screen. CPEBs are well known to be associated with LTM, where CPEB1 plays an established role in stimulating LTM-

https://doi.org/10.1021/acs.jproteome.4c00055
J. Proteome Res. 2025, 24, 27−45

and LTP/LTF-related *de novo* protein synthesis,[80,81] while CPEB2 has been shown to be required for both spatial memory in mice via its interaction with GRASP1[82] and in *Drosophila* long-term courtship memory, where the CPEB2 homologue is named Orb2.[83] Interestingly, similarly to EIF2D, upregulated CPEB2 in LTM may function to control the translation of specific transcripts key to LTM formation due to its ability to bind and stimulate translation of specific mRNA transcripts,[84] such as glutamate receptor interacting protein-associated protein 1 (GRASP1),[82] ephrin type-A receptor 4 (EphA4).[85] It would therefore be of interest to determine the expression of proteins under translational control of CPEB2 in the LTM and no LTM CNS to determine whether CPEB2 may regulate the expression of LTM-associated proteins, and compare these to noncanonical EIF2D-mediated translation.

While *de novo* protein synthesis and thus translation play key roles in the consolidation of LTM, so does specific ubiquitin-proteasome-mediated protein degradation. We identified proteins involved in ubiquitin-proteasome-mediated protein degradation as upregulated in LTM, such as HERC2/4, PSMB6, and PSMC2. These results are consistent with previous studies indicating the requirement of proteasome activity for LTM formation and LTP induction in various organisms[60,86−90] as well as previous results from our laboratory, where we used two-dimensional fluorescence difference in gel electrophoresis (2-D DIGE) approach to identify proteasome subunit β type-1 precursor as differentially expressed between LTM and yoke control CNS.[30] Other proteomic screens have also identified components of the proteasome to be upregulated by spatial learning, such as PSMB6 in rat dentate gyrus[8] and PSMA6 in mouse hippocampus.[67] Proteasome-mediated degradation appears to target ATF4, where inhibition of the proteasome leading to decreased ability to maintain late LTP also led to increased ATF4 immunoreactivity in hippocampal slices.[89] Thus, while eIF2D upregulation may result in subsequent ATF4 upregulation in LTM in this model, activity-dependent activation of the ubiquitin-proteasome complex may concomitantly degrade newly translated ATF4 stimulated by increased eIF2D activity, while potentially leaving other LTM-specific eIF2D targets intact. Interestingly, while the ubiquitin ligase HERC1 has been shown to be required for associative learning in mice,[91] previous studies on the effects of decreased HERC2, a ubiquitin ligase,[92] on LTM formation showed either no deficits, in heterozygous HERC2 knockout mice,[93] or better learning performance, in *Drosophila*.[94,95] HERC2 is further identified as a CrebB target gene.[95] As these data contrast with the results of the current screen, further investigation of the specific role of HERC2 in mediating LTM formation in this model and others is required.

Transcription. We identified a number of proteins as upregulated in LTM with functions involving transcription, consistent with the well-known requirement of transcription for LTM formation.[59,61] However, while LTM-associated transcription is well known to be dependent on activation of the transcription factor CREB, our screen identified nuclear transcription factor Y subunit γ (NFYC) as upregulated in LTM, a transcription factor responsible for transcription of many cell cycle proteins.[96−98] However, we did not identify any cell cycle proteins under the control of NFYC activity such as Cdc25, as associated with LTM (Table S2). Therefore, additional investigation is required to determine whether transcription general CCAAT-box promoter genes,[96] i.e., those under the control of NFYC, are associated with LTM formation in this model.

Due to a lack of availability of commercially available antibodies for *L. stagnalis*, biological validation of LTM-related changes in the expression of specific proteins was not conducted and represents a limitation of the data presented here. Screening for appropriate antibodies for candidate proteins based on sequence similarity presents a significant challenge, and due to the large number of candidate proteins identified in the current study, it will be a focus for future work. Individual proteins of interest could be verified by the generation of custom antibodies, especially for novel proteins identified in the current study. Furthermore, as relevant protein-coding sequences have been confirmed here as present in the *L. stagnalis* proteome, commercially available antibodies could be adapted for use in *L. stagnalis* based on protein sequences in order to verify changes in protein expression associated with LTM formation. It would be of additional interest to characterize the LTM, no LTM, and yoke CNS transcriptomes via RNaseq to quantify whole-brain transcript abundance and subsequently verify differentially expressed transcripts via qPCR, as we have done with LymEIF2D (Figure 6B). As mRNA and protein levels may not necessarily correlate when cells are not at steady-state[99,100] (i.e., during the memory consolidation process), RNaseq quantification and qPCR verification of differentially expressed mRNAs of candidate proteins identified in the current screen would provide a more thorough understanding of the molecular changes associated with consolidation.

Additionally, although many candidate proteins associated with LTM formation have been identified, it is still unclear which may be required for LTM formation. Previous studies have utilized RNA interference to knock down protein expression and assess effects on *L. stagnalis* behavior,[26,27,37,79,101−103] a promising approach for assessing if candidate proteins identified in the current proteomic screen are critical to LTM formation. Furthermore, as CRISPR/Cas9 gene editing has recently been developed for use in *L. stagnalis*,[104] it may be possible to identify the specific protein domains critical to LTM for previously identified or novel candidate LTM-associated proteins.

Novel *L. stagnalis* Proteins Associated with LTM Formation

While the current study focused on identifying potential functions of LTM-associated proteins with identified mouse homologues, as determined by protein−protein BLAST, 25/366 (6.83%) did not have a significant protein−protein BLAST hit in the mouse Uniprot proteome. The identities, closest homologues in other molluscan or invertebrate species, and inferred functions of these proteins would therefore be of interest for identifying potentially novel proteins critical to LTM with no conserved mammalian homologues or perhaps no conserved homologues whatsoever. Furthermore, though many proteins had a significant protein−protein BLAST hit to the mouse Uniprot proteome, many identified *Lymnaea* proteins had low (<30%) percentage identity to putative mouse homologues, suggesting that these proteins may have functions in addition to those inferred by sequence similarity. Future studies may therefore focus on phylogenetic and protein domain analyses of such proteins as well as the study of their *in vitro* and *in vivo* functions in *Lymnaea* to determine whether their functions are novel or conserved with mammalian proteins.

https://doi.org/10.1021/acs.jproteome.4c00055
J. Proteome Res. 2025, 24, 27−45

LTM Following Behavior Is Associated with Whole-CNS Changes in Protein Expression

We have demonstrated alterations in whole-CNS protein expression between LTM, no LTM, and yoke control animals, consistent with previous reports where whole-CNS inhibition of translation[25] and knockdown of expression of specific proteins critical to LTM[26,27] have been sufficient to eliminate LTM. Together with previous studies demonstrating similar whole-CNS alterations in protein expression associated with this model of LTM,[30,31] this suggests that a key element of LTM consolidation in this model is alterations in protein synthesis and thus neuronal properties in a large number of CNS neurons, in addition to the single CPG circuit, driven by the activity of the pacemaker neuron right pedal dorsal 1 (RPeD1), that is known to be the locus of LTM formation in this model.[105] While the activity of the central pattern generator circuit, particularly RPeD1, has been shown to be altered by LTM formation,[32,106] CPG neurons have projections throughout the CNS,[105,107] suggesting that activity-dependent changes in their output could lead to long-term modifications in activity CNS-wide. Recent studies on the *A. californica* have used single-neuron resolution voltage imaging to image activities of individual neurons[108] and to identify neuronal population activity dynamics associated with operant learning in isolated ganglia preparations.[109] A similar approach could be applied to *Lymnaea* to determine whether LTM-related changes in protein synthesis are reflected as whole-CNS changes in activity. Furthermore, droplet-based single-cell RNaseq[110] and proteomics[111] could be used to profile RNA and protein expression changes in individual neurons across the CNS using the *L. stagnalis* proteomic resource established in the current study and others.[58] Transcriptomes and proteomes of identified CPG neurons, such as RPeD1, could further be profiled and expression of transcripts and proteins, such as the large number of ion channels expressed in *L. stagnalis* CNS,[36] could be correlated with previously observed alterations in intrinsic and extrinsic neuronal properties of CPG neurons.

Our analyses identified 32 significantly differentially expressed proteins between LTM and no LTM CNS (Figure 2C), of which 8 did not differ significantly between no LTM and yoke controls (Table S2). These proteins were spermatogenesis-associated protein 13, serine palmitoyltransferase 2, partitioning defective 6 homologue γ, mitochondrial ribosome-associated GTPase 1, XK-related protein 6, dynamin-1-like, ATP-dependent (S)-NAD(P)H-hydrate dehydratase, and one protein (transcript ID: evgLocus_strawberry_AH_33731) which had no mouse homologue according to our criteria. While no clear pattern of function is evident within these proteins, of particular interest for subsequent investigation is serine palmitoyltransferase 2 (SPTLC2). Serine palmitoyltransferases are the rate-limiting enzyme complexes in ceramide synthesis,[112] where ceramide and its derivatives regulate a wide variety of neuronal functions, including AMPA and NMDA receptor function.[113] Therefore, increased expression of SPTLC2 specifically in LTM and not in no LTM animals, as we observed in our screen, may increase the availability of ceramides within the whole CNS, suggesting that it may be necessary for consolidation of LTM formation in this model.

Though the current study did not focus on the set of 330 unique proteins associated with the inability to form LTM (Supporting Figure 3C), the differential expression of these between no LTM and yoke control CNS implies that failure to acquire to LTM following aversive operant conditioning does not result in the activation of the same pathways as are associated with the yoking process. Indeed, the existence of differentially regulated proteins between yoke controls and no LTM CNS imply the existence of a "non-learned" or "learning-resistant" brain state that is distinct from simple exposure to hypoxia or aversive stimuli. Future work will examine the protein signaling pathways specifically associated with the failure to form LTM following aversive operant conditioning.

Comparison to Previous *L. stagnalis* LTM Proteomics Studies and Limitations

The current study identified 366 proteins associated with the ability to form LTM following aversive operant conditioning, a significant increase over the previous study, which identified approximately 40.[31] The current study directly utilized an *L. stagnalis*-specific predicted protein sequence library for protein identification followed by inference of function by sequence similarity, while the previous study used the Swiss Prot database for protein identification directly. Furthermore, while the previous study analyzed ganglia immediately following a third training session 24 h following aversive operant conditioning, our memory test did not involve administering aversive stimuli and thus did not reinforce LTM. The previous study also removed certain ganglia from the central ganglia preparation used for subsequent analysis while we looked at protein expression in the whole CNS. Finally, while our study used learning performance to segregate LTM from no LTM animals and compared with yoke control animals, the previous study compared LTM and yoke control or naïve animals. Therefore, as our protein set excludes proteins significantly regulated between no LTM and yoke control animals, some differentially expressed proteins may not overlap between these data sets.

Indeed, while several differentially expressed proteins potentially similar to those identified in the previous study were identified in our set of 366 LTM-associated proteins (proteins from the previous proteomic screen in parentheses), such as kinesin-1 heavy chain (kinesin-like protein KIF14), phosphatidylinositol 4-kinase α (phosphatidylinositol 4 phosphate 3 kinase C2 domain containing α polypeptide), cytochrome P450 2C44/3A11 (cytochrome P450 26A1), importin subunit α-4 (importin 9), and 39S ribosomal protein L4/L40, mitochondrial (39S ribosomal protein L17, mitochondrial), though without raw peptide sequences these comparisons may not be accurate. Importantly, we did not detect a significant upregulation of adenylate cyclase type 8 between the yoke control and LTM animals. However, as Western blot validation in the previous study demonstrated a significant difference in protein expression between LTM and naïve but not between LTM and yoke control ganglia, this suggests that potential differences may be difficult to detect. Furthermore, as our memory test did not involve a reinforcement-like step, it is possible that such stimulation may lead to short-term activity-dependent alterations in protein synthesis that may not have been triggered by our behavioral paradigm.

Notably, differences in identified proteins associated with LTM formation may be attributed to the possibility of false positives within our identified differentially expressed set, due to the assumption during our analyses that undetected proteins were truly absent from the sample, and therefore inherent bias within our data set toward high-abundance proteins. As we

https://doi.org/10.1021/acs.jproteome.4c00055
J. Proteome Res. 2025, 24, 27−45

have verified that at least one of our LTM-associated proteins, EIF2D, appears to be upregulated by aversive operant conditioning at least on the transcript level, we suggest that further verification of differentially expressed proteins associated with LTM be conducted by utilizing less resource-intensive methods such as qPCR prior to proceeding to more costly antibody-based verification of protein levels.

CONCLUSIONS

In conclusion, this study represents the first proteomic screen of LTM formation ability following aversive operant conditioning in *L. stagnalis* that takes advantage of a newly improved transcriptome-guided protein sequence library and collectively shows that LTM formation induces changes in the expression of proteins associated with protein synthesis, degradation, and transcription in this model. We have defined a set of 366 LTM-associated proteins and identified clusters of proteins with similar expression patterns between LTM, no LTM, and yoke controls, characterizing 88 as upregulated and 36 as downregulated in LTM, where upregulated proteins had significant functional enrichment for mRNA splicing and ubiquitin-mediated degradation pathways, suggesting that these pathways are upregulated by LTM formation in this model. Furthermore, our data identify, for the first time, a proposed *L. stagnalis* protein homologue of eukaryotic translation initiation factor 2D (LymEIF2D) and demonstrate upregulation of the corresponding transcript by aversive operant conditioning, suggesting that noncanonical translation initiation via EIF2D may play a role in promoting expression of LTM-specific proteins in this model. Our results further imply proteomic whole-brain states associated with successful LTM formation 24 h following aversive operant conditioning that are distinct from yoke controls. Further studies will explore the transcript levels of additional identified proteins and determine whether they are critical for LTM formation, hence using the current study as a jumping off point for a more detailed exploration of a diverse set of protein signaling pathways and their involvement in LTM. Analysis of whole CNS and specific neural activity associated with LTM-related alterations in protein signaling identified in the current study will lead to the discovery of novel mechanisms of regulation of neuronal function in learning and memory.

ASSOCIATED CONTENT

Data Availability Statement

Raw MS data has been deposited to MassIVE at the following URL: ftp://massive.ucsd.edu/v07/MSV000094487/.

Supporting Information

The Supporting Information is available free of charge at https://pubs.acs.org/doi/10.1021/acs.jproteome.4c00055.

Comparison of identification of *Lymnaea stagnalis* proteins from raw mass spectrometry output files between MaxQuant and DIA-NN (Supporting Figure 1); distribution of $-\log_{10}$ *e*-values for mouse homologues of *L. stagnalis* CNS proteins (Supporting Figure 2); volcano plots of LTM vs no LTM, LTM vs yoke control, and no LTM vs yoke control differentially expressed proteins (Supporting Figure 3); biological process GO terms in LTM-associated differentially regulated protein set (Supporting Figure 4); molecular function GO terms in LTM-associated differentially regulated protein set (Supporting Figure 5); and cellular component GO terms in LTM-associated differentially regulated protein set (Supporting Figure 6) (PDF)

MaxLFQ data for each LTM, no LTM, and yoke control CNS samples (averaged by technical replicate) (XLS)

Processed log 2 MaxLFQ data across all LTM, no LTM, and yoke control CNS samples (XLS)

Differential expression and protein group identification of significant proteins associated with LTM formation (PDF)

AUTHOR INFORMATION

Corresponding Author

Zhong-Ping Feng − *Department of Physiology, University of Toronto, Toronto, Ontario M5S 1A8, Canada*; orcid.org/0000-0002-2454-4462; Email: zp.feng@utoronto.ca

Authors

Julia Bandura − *Department of Physiology, University of Toronto, Toronto, Ontario M5S 1A8, Canada*

Calvin Chan − *Department of Chemistry, University of Toronto, Toronto, Ontario M5S 3H6, Canada*; orcid.org/0000-0003-0640-0921

Hong-Shuo Sun − *Department of Surgery, University of Toronto, Toronto, Ontario M5S 1A1, Canada*

Aaron R. Wheeler − *Department of Chemistry, University of Toronto, Toronto, Ontario M5S 3H6, Canada; Donnelly Centre for Cellular and Biomedical Research, University of Toronto, Toronto, Ontario M5S 3E1, Canada; Institute of Biomedical Engineering, University of Toronto, Toronto, Ontario M5S 3E2, Canada*; orcid.org/0000-0001-5230-7475

Complete contact information is available at: https://pubs.acs.org/10.1021/acs.jproteome.4c00055

Notes

The authors declare no competing financial interest.

ACKNOWLEDGMENTS

This work was supported by Canadian Institutes of Health Research (CIHR) (PJT-153155) to Z.-P.F., Natural Sciences and Engineering Research Council of Canada (NSERC) (RGPIN-2022-04467 to Z.-P.F., RGPIN-2022-04574 to H.-S.S., RGPIN 2019-04867 to A.R.W.), and the Canadian Foundation for Innovation/Province of Ontario to A.R.W. J.B. is a recipient of the NSERC postgraduate scholarship (PGS-D) and Ontario Graduate Scholarship (OGS-D).

ABBREVIATIONS

5-HT:5-hydroxytryptamine
ATF4:activating transcription factor 4
BLAST:basic local alignment tool
BP:biological process
cAMP:cyclic adenosine monophosphate
CC:cellular compartment
CNS:central nervous system
CPEB2:cytoplasmic polyadenylation element binding 2
CPG:central pattern generator
CREB1:calcium/cAMP-response element-binding protein 1
eIF2D:eukaryotic translation initiation factor 2D
FC:fold change
FDR:false discovery rate

https://doi.org/10.1021/acs.jproteome.4c00055
J. Proteome Res. 2025, 24, 27−45

GO:gene ontology
LC:liquid chromatography
LC-MS:liquid chromatography-mass spectrometry
LTM:long-term memory
MAPK:mitogen-activated protein kinase
MEN1:multiple endocrine neoplasia type 1
MF:molecular function
MS:mass spectrometry
MT:memory test
NMDA:*N*-methyl-D-aspartate
PT:pretest

REFERENCES

(1) Bourtchouladze, R.; Abel, T.; Berman, N.; Gordon, R.; Lapidus, K.; Kandel, E. R. Different Training Procedures Recruit Either One or Two Critical Periods for Contextual Memory Consolidation, Each of Which Requires Protein Synthesis and PKA. *Learn. Mem.* **1998**, *5* (4), 365−374.

(2) Davis, H. P.; Squire, L. R. Protein Synthesis and Memory: A Review. *Psychol. Bull.* **1984**, *96* (3), 518−559.

(3) Quevedo, J.; Vianna, M. R. M.; Martins, M. R.; Barichello, T.; Medina, J. H.; Roesler, R.; Izquierdo, I. Protein Synthesis, PKA, and MAP Kinase Are Differentially Involved in Short- and Long-Term Memory in Rats. *Behav. Brain Res.* **2004**, *154* (2), 339−343.

(4) Klann, E.; Sweatt, J. D. Altered Protein Synthesis Is a Trigger for Long-Term Memory Formation. *Neurobiol. Learn. Mem.* **2008**, *89* (3), 247−259.

(5) Costa-Mattioli, M.; Sossin, W. S.; Klann, E.; Sonenberg, N. Translational Control of Long-Lasting Synaptic Plasticity and Memory. *Neuron* **2009**, *61* (1), 10−26.

(6) Costa-Mattioli, M.; Klann, E. Translational Control Mechanisms in Synaptic Plasticity and Memory. *Curated Ref. Collect. Neurosci. Biobehav. Psychol.* **2017**, *61* (1), 311−328.

(7) Borovok, N.; Nesher, E.; Levin, Y.; Reichenstein, M.; Pinhasov, A.; Michaelevski, I. Dynamics of Hippocampal Protein Expression During Long-Term Spatial Memory Formation. *Mol. Cell. Proteomics* **2016**, *15* (2), 523−541.

(8) Monopoli, M. P.; Raghnaill, M. N.; Loscher, J. S.; O'Sullivan, N. C.; Pangalos, M. N.; Ring, R. H.; von Schack, D.; Dunn, M. J.; Regan, C. M.; Pennington, S.; Murphy, K. J. Temporal Proteomic Profile of Memory Consolidation in the Rat Hippocampal Dentate Gyrus. *Proteomics* **2011**, *11* (21), 4189−4201.

(9) Hong, I.; Kang, T.; Yun, K. N.; Yoo, Y.; Park, S.; Kim, J.; An, B.; Song, S.; Lee, S.; Kim, J.; Song, B.; Kwon, K.-H.; Kim, J. Y.; Park, Y. M.; Choi, S. Quantitative Proteomics of Auditory Fear Conditioning. *Biochem. Biophys. Res. Commun.* **2013**, *434* (1), 87−94.

(10) Šmidák, R.; Mayer, R. L.; Bileck, A.; Gerner, C.; Mechtcheriakova, D.; Stork, O.; Lubec, G.; Li, L. Quantitative Proteomics Reveals Protein Kinases and Phosphatases in the Individual Phases of Contextual Fear Conditioning in the C57BL/6J Mouse. *Behav. Brain Res.* **2016**, *303*, 208−217.

(11) Farrell, K.; Musaus, M.; Navabpour, S.; Martin, K.; Ray, W. K.; Helm, R. F.; Jarome, T. J. Proteomic Analysis Reveals Sex-Specific Protein Degradation Targets in the Amygdala During Fear Memory Formation. *Front. Mol. Neurosci.* **2021**, *14*, No. 716284, DOI: 10.3389/fnmol.2021.716284.

(12) Gaiardo, R. B.; Pedroso, A. P.; Ribeiro, E. B.; Tashima, A. K.; Telles, M. M.; Cerutti, S. M. Proteome Analysis Indicates Participation of the Dorsal Hippocampal Formation in Fear-Motivated Memory in a Time-Dependent Manner. *Behav. Neurosci.* **2023**, *137* (5), 303−318.

(13) Rao-Ruiz, P.; Carney, K. E.; Pandya, N.; van der Loo, R. J.; Verheijen, M. H. G.; van Nierop, P.; Smit, A. B.; Spijker, S. Time-Dependent Changes in the Mouse Hippocampal Synaptic Membrane Proteome after Contextual Fear Conditioning. *Hippocampus* **2015**, *25* (11), 1250−1261.

(14) Kähne, T.; Kolodziej, A.; Smalla, K.; Eisenschmidt, E.; Haus, U.; Weismantel, R.; Kropf, S.; Wetzel, W.; Ohl, F. W.; Tischmeyer, W.; Naumann, M.; Gundelfinger, E. D. Synaptic Proteome Changes in Mouse Brain Regions upon Auditory Discrimination Learning. *Proteomics* **2012**, *12* (15−16), 2433−2444.

(15) Kähne, T.; Richter, S.; Kolodziej, A.; Smalla, K.-H.; Pielot, R.; Engler, A.; Ohl, F. W.; Dieterich, D. C.; Seidenbecher, C.; Tischmeyer, W.; Naumann, M.; Gundelfinger, E. D. Proteome Rearrangements after Auditory Learning: High-Resolution Profiling of Synapse-Enriched Protein Fractions from Mouse Brain. *J. Neurochem.* **2016**, *138* (1), 124−138.

(16) Kim, Y. G.; Woo, J.; Park, J.; Kim, S.; Lee, Y.-S.; Kim, Y.; Kim, S. J. Quantitative Proteomics Reveals Distinct Molecular Signatures of Different Cerebellum-Dependent Learning Paradigms. *J. Proteome Res.* **2020**, *19* (5), 2011−2025.

(17) Jiang, H.; Hou, Q.; Gong, Z.; Liu, L. Proteomic and Transcriptomic Analysis of Visual Long-Term Memory in Drosophila Melanogaster. *Protein Cell* **2011**, *2* (3), 215−222.

(18) Zhang, Y.; Shan, B.; Boyle, M.; Liu, J.; Liao, L.; Xu, T.; Yates, J. R. I. Brain Proteome Changes Induced by Olfactory Learning in Drosophila. *J. Proteome Res.* **2014**, *13* (8), 3763−3770.

(19) Lee, T.-R.; Lee, H.-Y.; Huang, S.-H.; Chan, H.-T.; Lyu, P.-C.; Chan, H.-L. Comparative Proteomics Analysis of Normal and Memory-Deficient Drosophila Melanogaster Heads. *Zool. Stud.* **2013**, *52* (1), No. 10.

(20) Monje, F. J.; Birner-Gruenberger, R.; Darnhofer, B.; Divisch, I.; Pollak, D. D.; Lubec, G. Proteomics Reveals Selective Regulation of Proteins in Response to Memory-Related Serotonin Stimulation in Aplysia Californica Ganglia. *Proteomics* **2012**, *12* (3), 490−499.

(21) Crow, T.; Xue-Bian, J.-J. Proteomic Analysis of Short- and Intermediate-Term Memory in Hermissenda. *Neuroscience* **2011**, *192*, 102−111.

(22) Lukowiak, K.; Ringseis, E.; Spencer, G.; Wildering, W.; Syed, N. Operant Conditioning of Aerial Respiratory Behaviour in Lymnaea Stagnalis. *J. Exp. Biol.* **1996**, *199* (Pt 3), 683−691.

(23) Lukowiak, K.; Cotter, R.; Westly, J.; Ringseis, E.; Spencer, G.; Syed, N. Long-Term Memory of an Operantly Conditioned Respiratory Behaviour Pattern in Lymnaea Stagnalis. *J. Exp. Biol.* **1998**, *201* (6), 877−882.

(24) Sangha, S.; Scheibenstock, A.; Lukowiak, K. Reconsolidation of a Long-Term Memory in Lymnaea Requires New Protein and RNA Synthesis and the Soma of Right Pedal Dorsal 1. *J. Neurosci.* **2003**, *23* (22), 8034−8040.

(25) Sangha, S.; Scheibenstock, A.; McComb, C.; Lukowiak, K. Intermediate and Long-Term Memories of Associative Learning Are Differentially Affected by Transcription versus Translation Blockers in Lymnaea. *J. Exp. Biol.* **2003**, *206* (10), 1605−1613.

(26) Dong, N.; Senzel, A.; Li, K.; Lu, T. Z.; Guo, C. H.; Aleksic, M.; Feng, Z. P. MEN1 Tumor Suppressor Gene Is Required for Long-Term Memory Formation in an Aversive Operant Conditioning Model of Lymnaea Stagnalis. *Neuroscience* **2018**, *379*, 22−31.

(27) Guo, C.-H.; Senzel, A.; Li, K.; Feng, Z.-P. De Novo Protein Synthesis of Syntaxin-1 and Dynamin-1 in Long-Term Memory Formation Requires CREB1 Gene Transcription in Lymnaea Stagnalis. *Behav. Genet.* **2010**, *40* (5), 680−693.

(28) Rosenegger, D.; Lukowiak, K. The Participation of NMDA Receptors, PKC, and MAPK in the Formation of Memory Following Operant Conditioning in Lymnaea. *Mol. Brain* **2010**, *3* (1), 24.

(29) Silverman-Gavrila, L. B.; Lu, T. Z.; Prashad, R. C.; Nejatbakhsh, N.; Charlton, M. P.; Feng, Z. P. Neural Phosphoproteomics of a Chronic Hypoxia Model-Lymnaea Stagnalis. *Neuroscience* **2009**, *161* (2), 621−634.

(30) Silverman-Gavrila, L. B.; Senzel, A. G.; Charlton, M. P.; Feng, Z. P. Expression, Phosphorylation, and Glycosylation of CNS Proteins in Aversive Operant Conditioning Associated Memory in Lymnaea Stagnalis. *Neuroscience* **2011**, *186*, 94−109.

(31) Rosenegger, D.; Wright, C.; Lukowiak, K. A Quantitative Proteomic Analysis of Long-Term Memory. *Mol. Brain* **2010**, *3* (1), No. 9.

(32) Dong, N.; Feng, Z. P. Inverse Relationship between Basal Pacemaker Neuron Activity and Aversive Long-Term Memory

https://doi.org/10.1021/acs.jproteome.4c00055
J. Proteome Res. 2025, 24, 27−45

Formation in Lymnaea Stagnalis. *Front. Cell. Neurosci.* **2017**, *10*, No. 297.
(33) Feng, Z. P.; Zhang, Z.; van Kesteren, R. E.; Straub, V. A.; van Nierop, P.; Jin, K.; Nejatbakhsh, N.; Goldberg, J. I.; Spencer, G. E.; Yeoman, M. S.; Wildering, W.; Coorssen, J. R.; Croll, R. P.; Buck, L. T.; Syed, N. I.; Smit, A. B. Transcriptome Analysis of the Central Nervous System of the Mollusc Lymnaea Stagnalis. *BMC Genomics* **2009**, *10*, 451.
(34) Sadamoto, H.; Takahashi, H.; Okada, T.; Kenmoku, H.; Toyota, M.; Asakawa, Y. De Novo Sequencing and Transcriptome Analysis of the Central Nervous System of Mollusc Lymnaea Stagnalis by Deep RNA Sequencing. *PLoS One* **2012**, *7* (8), No. e42546.
(35) Rosato, M.; Hoelscher, B.; Lin, Z.; Agwu, C.; Xu, F. Transcriptome Analysis Provides Genome Annotation and Expression Profiles in the Central Nervous System of Lymnaea Stagnalis at Different Ages. *BMC Genomics* **2021**, *22*, No. 637, DOI: 10.1186/s12864-021-07946-y.
(36) Dong, N.; Bandura, J.; Zhang, Z.; Wang, Y.; Labadie, K.; Noel, B.; Davison, A.; Koene, J. M.; Sun, H.-S.; Coutellec, M.-A.; Feng, Z.-P. Ion Channel Profiling of the Lymnaea Stagnalis Ganglia via Transcriptome Analysis. *BMC Genomics* **2021**, *22* (1), No. 18, DOI: 10.1186/s12864-020-07287-2.
(37) Fei, G.; Guo, C.; Sun, H. S.; Feng, Z. P. Chronic Hypoxia Stress-Induced Differential Modulation of Heat-Shock Protein 70 and Presynaptic Proteins. *J. Neurochem.* **2007**, *100* (1), 50−61.
(38) Elliott, C. J.; Benjamin, P. R. Esophageal Mechanoreceptors in the Feeding System of the Pond Snail, Lymnaea Stagnalis. *J. Neurophysiol.* **1989**, *61* (4), 727−736.
(39) Han, C.-L.; Chien, C.-W.; Chen, W.-C.; Chen, Y.-R.; Wu, C.-P.; Li, H.; Chen, Y.-J. A Multiplexed Quantitative Strategy for Membrane Proteomics: Opportunities for Mining Therapeutic Targets for Autosomal Dominant Polycystic Kidney Disease. *Mol. Cell. Proteomics* **2008**, *7* (10), 1983−1997.
(40) Demichev, V.; Messner, C. B.; Vernardis, S. I.; Lilley, K. S.; Ralser, M. DIA-NN: Neural Networks and Interference Correction Enable Deep Proteome Coverage in High Throughput. *Nat. Methods* **2020**, *17* (1), 41−44.
(41) Cox, J.; Matic, I.; Hilger, M.; Nagaraj, N.; Selbach, M.; Olsen, J. V.; Mann, M. A Practical Guide to the Maxquant Computational Platform for Silac-Based Quantitative Proteomics. *Nat. Protoc.* **2009**, *4* (5), 698−705.
(42) Tyanova, S.; Temu, T.; Cox, J. The MaxQuant Computational Platform for Mass Spectrometry-Based Shotgun Proteomics. *Nat. Protoc.* **2016**, *11* (12), 2301−2319.
(43) Zhang, X.; Smits, A. H.; Van Tilburg, G. B.; Ovaa, H.; Huber, W.; Vermeulen, M. Proteome-Wide Identification of Ubiquitin Interactions Using UbIA-MS. *Nat. Protoc.* **2018**, *13* (3), 530−550.
(44) Altschul, S. F.; Gish, W.; Miller, W.; Myers, E. W.; Lipman, D. J. Basic Local Alignment Search Tool. *J. Mol. Biol.* **1990**, *215* (3), 403−410.
(45) The UniProt Consortium. UniProt: The Universal Protein Knowledgebase in 2023. *Nucleic Acids Res.* **2023**, *51* (D1), D523−D531, DOI: 10.1093/nar/gkac1052.
(46) Supek, F.; Bošnjak, M.; Škunca, N.; Šmuc, T. REVIGO Summarizes and Visualizes Long Lists of Gene Ontology Terms. *PLoS One* **2011**, *6* (7), No. e21800.
(47) Wickham, H. *Ggplot2; Use R!*; Springer International Publishing: Cham, 2016.
(48) Shannon, P.; Markiel, A.; Ozier, O.; Baliga, N. S.; Wang, J. T.; Ramage, D.; Amin, N.; Schwikowski, B.; Ideker, T. Cytoscape: A Software Environment for Integrated Models of Biomolecular Interaction Networks. *Genome Res.* **2003**, *13* (11), 2498−2504.
(49) Fernandez, N. F.; Gundersen, G. W.; Rahman, A.; Grimes, M. L.; Rikova, K.; Hornbeck, P.; Ma'ayan, A. Clustergrammer, a Web-Based Heatmap Visualization and Analysis Tool for High-Dimensional Biological Data. *Sci. Data* **2017**, *4* (1), No. 170151.
(50) Szklarczyk, D.; Franceschini, A.; Wyder, S.; Forslund, K.; Heller, D.; Huerta-Cepas, J.; Simonovic, M.; Roth, A.; Santos, A.; Tsafou, K. P.; Kuhn, M.; Bork, P.; Jensen, L. J.; Mering, V. STRING V10: Protein−Protein Interaction Networks, Integrated over the Tree of Life. *Nucleic Acids Res.* **2015**, *43* (D1), D447−D452.
(51) Doncheva, N. T.; Morris, J. H.; Gorodkin, J.; Jensen, L. J. Cytoscape StringApp: Network Analysis and Visualization of Proteomics Data. *J. Proteome Res.* **2019**, *18* (2), 623−632.
(52) Chen, E. Y.; Tan, C. M.; Kou, Y.; Duan, Q.; Wang, Z.; Meirelles, G. V.; Clark, N. R.; Ma'ayan, A. Enrichr: Interactive and Collaborative HTML5 Gene List Enrichment Analysis Tool. *BMC Bioinf.* **2013**, *14*, No. 128.
(53) Kuleshov, M. V.; Jones, M. R.; Rouillard, A. D.; Fernandez, N. F.; Duan, Q.; Wang, Z.; Koplev, S.; Jenkins, S. L.; Jagodnik, K. M.; Lachmann, A.; McDermott, M. G.; Monteiro, C. D.; Gundersen, G. W.; Ma'ayan, A. Enrichr: A Comprehensive Gene Set Enrichment Analysis Web Server 2016 Update. *Nucleic Acids Res.* **2016**, *44* (W1), W90−W97.
(54) Xie, Z.; Bailey, A.; Kuleshov, M. V.; Clarke, D. J. B.; Evangelista, J. E.; Jenkins, S. L.; Lachmann, A.; Wojciechowicz, M. L.; Kropiwnicki, E.; Jagodnik, K. M.; Jeon, M.; Ma'ayan, A. Gene Set Knowledge Discovery with Enrichr. *Curr. Protoc.* **2021**, *1* (3), No. e90.
(55) Notredame, C.; Higgins, D. G.; Heringa, J. T-Coffee: A Novel Method for Fast and Accurate Multiple Sequence Alignment. *J. Mol. Biol.* **2000**, *302* (1), 205−217.
(56) Waterhouse, A. M.; Procter, J. B.; Martin, D. M. A.; Clamp, M.; Barton, G. J. Jalview Version 2-A Multiple Sequence Alignment Editor and Analysis Workbench. *Bioinformatics* **2009**, *25*, 1189.
(57) Jones, P.; Binns, D.; Chang, H. Y.; Fraser, M.; Li, W.; McAnulla, C.; McWilliam, H.; Maslen, J.; Mitchell, A.; Nuka, G.; Pesseat, S.; Quinn, A. F.; Sangrador-Vegas, A.; Scheremetjew, M.; Yong, S. Y.; Lopez, R.; Hunter, S. InterProScan 5: Genome-Scale Protein Function Classification. *Bioinformatics* **2014**, *30* (9), 1236−1240.
(58) Wooller, S.; Anagnostopoulou, A.; Kuropka, B.; Crossley, M.; Benjamin, P. R.; Pearl, F.; Kemenes, I.; Kemenes, G.; Eravci, M. A Combined Bioinformatics and LC-MS-Based Approach for the Development and Benchmarking of a Comprehensive Database of *Lymnaea* CNS Proteins. *J. Exp. Biol.* **2022**, *225* (7), No. jeb243753.
(59) Rainbow, T. C. Role of RNA and Protein Synthesis in Memory Formation. *Neurochem. Res.* **1979**, *4* (3), 297−312.
(60) Lyons, L. C.; Gardner, J. S.; Gandour, C. E.; Krishnan, H. C. Role of Proteasome-Dependent Protein Degradation in Long-Term Operant Memory in Aplysia. *Learn. Mem.* **2017**, *24* (1), 59−64.
(61) Hawkins, R. D.; Kandel, E. R.; Bailey, C. H. Molecular Mechanisms of Memory Storage in Aplysia. *Biol. Bull.* **2006**, *210* (3), 174−191.
(62) Bourtchuladze, R.; Frenguelli, B.; Blendy, J.; Cioffi, D.; Schutz, G.; Silva, A. J. Deficient Long-Term Memory in Mice with a Targeted Mutation of the cAMP-Responsive Element-Binding Protein. *Cell* **1994**, *79* (1), 59−68.
(63) Mayford, M.; Bach, M. E.; Huang, Y. Y.; Wang, L.; Hawkins, R. D.; Kandel, E. R. Control of Memory Formation through Regulated Expression of a CaMKII Transgene. *Science* **1996**, *274* (5293), 1678−1683.
(64) Yin, J. C.; Tully, T. CREB and the Formation of Long-Term Memory. *Curr. Opin. Neurobiol.* **1996**, *6* (2), 264−268.
(65) Abel, T.; Nguyen, P. V.; Barad, M.; Deuel, T. A. S.; Kandel, E. R.; Bourtchouladze, R. Genetic Demonstration of a Role for PKA in the Late Phase of LTP and in Hippocampus-Based Long-Term Memory. *Cell* **1997**, *88* (5), 615−626.
(66) Bartsch, D.; Casadio, A.; Karl, K. A.; Serodio, P.; Kandel, E. R. CREB1 Encodes a Nuclear Activator, a Repressor, and a Cytoplasmic Modulator That Form a Regulatory Unit Critical for Long-Term Facilitation. *Cell* **1998**, *95* (2), 211−223.
(67) Borovok, N.; Nesher, E.; Levin, Y.; Reichenstein, M.; Pinhasov, A.; Michaelevski, I. Dynamics of Hippocampal Protein Expression During Long-Term Spatial Memory Formation. *Mol. Cell. Proteomics* **2016**, 523−541, DOI: 10.1074/mcp.M115.051318.
(68) Costa-Mattioli, M.; Gobert, D.; Harding, H.; Herdy, B.; Azzi, M.; Bruno, M.; Bidinosti, M.; Ben Mamou, C.; Marcinkiewicz, E.;

Yoshida, M.; Imataka, H.; Cuello, A. C.; Seidah, N.; Sossin, W.; Lacaille, J.-C.; Ron, D.; Nader, K.; Sonenberg, N. Translational Control of Hippocampal Synaptic Plasticity and Memory by the eIF2α Kinase GCN2. *Nature* **2005**, *436* (7054), 1166−1170.
(69) Costa-Mattioli, M.; Gobert, D.; Stern, E.; Gamache, K.; Colina, R.; Cuello, C.; Sossin, W.; Kaufman, R.; Pelletier, J.; Rosenblum, K.; Krnjević, K.; Lacaille, J.-C.; Nader, K.; Sonenberg, N. eIF2α Phosphorylation Bidirectionally Regulates the Switch from Short- to Long-Term Synaptic Plasticity and Memory. *Cell* **2007**, *129* (1), 195−206.
(70) Gkogkas, C.; Sonenberg, N.; Costa-Mattioli, M. Translational Control Mechanisms in Long-Lasting Synaptic Plasticity and Memory. *J. Biol. Chem.* **2010**, *285* (42), 31913−31917.
(71) Panchision, D. M.; Gerwin, C. M.; DeLorenzo, R. J.; Jakoi, E. R. Glutamate Receptor Activation Regulates mRNA at Both Transcriptional and Posttranscriptional Levels. *J. Neurochem.* **1995**, *65* (3), 969−977.
(72) Schleich, S.; Strassburger, K.; Janiesch, P. C.; Koledachkina, T.; Miller, K. K.; Haneke, K.; Cheng, Y.-S.; Küchler, K.; Stoecklin, G.; Duncan, K. E.; Teleman, A. A. DENR−MCT-1 Promotes Translation Re-Initiation Downstream of uORFs to Control Tissue Growth. *Nature* **2014**, *512* (7513), 208−212.
(73) Dmitriev, S. E.; Terenin, I. M.; Andreev, D. E.; Ivanov, P. A.; Dunaevsky, J. E.; Merrick, W. C.; Shatsky, I. N. GTP-Independent tRNA Delivery to the Ribosomal P-Site by a Novel Eukaryotic Translation Factor. *J. Biol. Chem.* **2010**, *285* (35), 26779−26787.
(74) Sonobe, Y.; Aburas, J.; Krishnan, G.; Fleming, A. C.; Ghadge, G.; Islam, P.; Warren, E. C.; Gu, Y.; Kankel, M. W.; Brown, A. E. X.; Kiskinis, E.; Gendron, T. F.; Gao, F.-B.; Roos, R. P.; Kratsios, P. A C. Elegans Model of C9orf72-Associated ALS/FTD Uncovers a Conserved Role for eIF2D in RAN Translation. *Nat. Commun.* **2021**, *12* (1), No. 6025.
(75) Green, K. M.; Miller, S. L.; Malik, I.; Todd, P. K. Non-Canonical Initiation Factors Modulate Repeat-Associated Non-AUG Translation. *Hum. Mol. Genet.* **2022**, *31* (15), 2521−2534.
(76) Vasudevan, D.; Neuman, S. D.; Yang, A.; Lough, L.; Brown, B.; Bashirullah, A.; Cardozo, T.; Ryoo, H. D. Translational Induction of ATF4 during Integrated Stress Response Requires Noncanonical Initiation Factors eIF2D and DENR. *Nat. Commun.* **2020**, *11* (1), No. 4677.
(77) Bartsch, D.; Ghirardi, M.; Skehel, P. A.; Karl, K. A.; Herder, S. P.; Chen, M.; Bailey, C. H.; Kandel, E. R. Aplysia CREB2 Represses Long-Term Facilitation: Relief of Repression Converts Transient Facilitation into Long-Term Functional and Structural Change. *Cell* **1995**, *83* (6), 979−992.
(78) Chen, A.; Muzzio, I. A.; Malleret, G.; Bartsch, D.; Verbitsky, M.; Pavlidis, P.; Yonan, A. L.; Vronskaya, S.; Grody, M. B.; Cepeda, I.; Gilliam, T. C.; Kandel, E. R. Inducible Enhancement of Memory Storage and Synaptic Plasticity in Transgenic Mice Expressing an Inhibitor of ATF4 (CREB-2) and C/EBP Proteins. *Neuron* **2003**, *39* (4), 655−669.
(79) Korneev, S. A.; Vavoulis, D. V.; Naskar, S.; Dyakonova, V. E.; Kemenes, I.; Kemenes, G. A CREB2-Targeting microRNA Is Required for Long-Term Memory after Single-Trial Learning. *Sci. Rep.* **2018**, *8* (1), No. 3950.
(80) Si, K.; Giustetto, M.; Etkin, A.; Hsu, R.; Janisiewicz, A. M.; Miniaci, M. C.; Kim, J.-H.; Zhu, H.; Kandel, E. R. A Neuronal Isoform of CPEB Regulates Local Protein Synthesis and Stabilizes Synapse-Specific Long-Term Facilitation in Aplysia. *Cell* **2003**, *115* (7), 893−904.
(81) Miniaci, M. C.; Kim, J.-H.; Puthanveettil, S. V.; Si, K.; Zhu, H.; Kandel, E. R.; Bailey, C. H. Sustained CPEB-Dependent Local Protein Synthesis Is Required to Stabilize Synaptic Growth for Persistence of Long-Term Facilitation in Aplysia. *Neuron* **2008**, *59* (6), 1024−1036.
(82) Lu, W.-H.; Yeh, N.-H.; Huang, Y.-S. CPEB2 Activates GRASP1 mRNA Translation and Promotes AMPA Receptor Surface Expression, Long-Term Potentiation, and Memory. *Cell Rep.* **2017**, *21* (7), 1783−1794.
(83) Keleman, K.; Krüttner, S.; Alenius, M.; Dickson, B. J. Function of the Drosophila CPEB Protein Orb2 in Long-Term Courtship Memory. *Nat. Neurosci.* **2007**, *10* (12), 1587−1593.
(84) Huang, Y.-S.; Kan, M.; Lin, C.; Richter, J. D. CPEB3 and CPEB4 in Neurons: Analysis of RNA-binding Specificity and Translational Control of AMPA Receptor GluR2 mRNA. *EMBO J.* **2006**, *25* (20), 4865−4876.
(85) Turimella, S. L.; Bedner, P.; Skubal, M.; Vangoor, V. R.; Kaczmarczyk, L.; Karl, K.; Zoidl, G.; Gieselmann, V.; Seifert, G.; Steinhäuser, C.; Kandel, E.; Theis, M. Characterization of Cytoplasmic Polyadenylation Element Binding 2 Protein Expression and Its RNA Binding Activity. *Hippocampus* **2015**, *25* (5), 630−642.
(86) Chain, D. G.; Casadio, A.; Schacher, S.; Hegde, A. N.; Valbrun, M.; Yamamoto, N.; Goldberg, A. L.; Bartsch, D.; Kandel, E. R.; Schwartz, J. H. Mechanisms for Generating the Autonomous cAMP-Dependent Protein Kinase Required for Long-Term Facilitation in Aplysia. *Neuron* **1999**, *22* (1), 147−156.
(87) Lopez-Salon, M.; Alonso, M.; Vianna, M. R. M.; Viola, H.; E Souza, T. M.; Izquierdo, I.; Pasquini, J. M.; Medina, J. H. The Ubiquitin−Proteasome Cascade Is Required for Mammalian Long-Term Memory Formation. *Eur. J. Neurosci.* **2001**, *14* (11), 1820−1826.
(88) Merlo, E.; Romano, A. Long-Term Memory Consolidation Depends on Proteasome Activity in the Crab Chasmagnathus. *Neuroscience* **2007**, *147* (1), 46−52.
(89) Dong, C.; Upadhya, S. C.; Ding, L.; Smith, T. K.; Hegde, A. N. Proteasome Inhibition Enhances the Induction and Impairs the Maintenance of Late-Phase Long-Term Potentiation. *Learn. Mem.* **2008**, *15* (5), 335−347.
(90) Jarome, T. J.; Werner, C. T.; Kwapis, J. L.; Helmstetter, F. J. Activity Dependent Protein Degradation Is Critical for the Formation and Stability of Fear Memory in the Amygdala. *PLoS One* **2011**, *6* (9), No. e24349.
(91) Pérez-Villegas, E. M.; Pérez-Rodríguez, M.; Negrete-Díaz, J. V.; Ruiz, R.; Rosa, J. L.; de Toledo, G. A.; Rodríguez-Moreno, A.; Armengol, J. A. HERC1 Ubiquitin Ligase Is Required for Hippocampal Learning and Memory. *Front. Neuroanat.* **2020**, *14*, No. 592797, DOI: 10.3389/fnana.2020.592797.
(92) Martínez-Noël, G.; Luck, K.; Kühnle, S.; Desbuleux, A.; Szajner, P.; Galligan, J. T.; Rodriguez, D.; Zheng, L.; Boyland, K.; Leclere, F.; Zhong, Q.; Hill, D. E.; Vidal, M.; Howley, P. M. Network Analysis of UBE3A/E6AP-Associated Proteins Provides Connections to Several Distinct Cellular Processes. *J. Mol. Biol.* **2018**, *430* (7), 1024−1050.
(93) Cubillos-Rojas, M.; Schneider, T.; Hadjebi, O.; Pedrazza, L.; de Oliveira, J. R.; Langa, F.; Guénet, J.-L.; Duran, J.; de Anta, J. M.; Alcántara, S.; Ruiz, R.; Pérez-Villegas, E. M.; Aguilar, F. J.; Carrión, Á. M.; Armengol, J. A.; Baple, E.; Crosby, A. H.; Bartrons, R.; Ventura, F.; Rosa, J. L. The HERC2 Ubiquitin Ligase Is Essential for Embryonic Development and Regulates Motor Coordination. *Oncotarget* **2016**, *7* (35), 56083−56106.
(94) Walkinshaw, E.; Gai, Y.; Farkas, C.; Richter, D.; Nicholas, E.; Keleman, K.; Davis, R. L. Identification of Genes That Promote or Inhibit Olfactory Memory Formation in *Drosophila*. *Genetics* **2015**, *199* (4), 1173−1182.
(95) Sgammeglia, N.; Widmer, Y. F.; Kaldun, J. C.; Fritsch, C.; Bruggmann, R.; Sprecher, S. G. Memory Phase-Specific Genes in the Mushroom Bodies Identified Using CrebB-Target DamID. *PLoS Genet.* **2023**, *19* (6), No. e1010802.
(96) Mantovani, R. The Molecular Biology of the CCAAT-Binding Factor NF-Y. *Gene* **1999**, *239* (1), 15−27.
(97) Zwicker, J.; Lucibello, F. C.; Wolfraim, L. A.; Gross, C.; Truss, M.; Engeland, K.; Müller, R. Cell Cycle Regulation of the Cyclin A, cdc25C and Cdc2 Genes Is Based on a Common Mechanism of Transcriptional Repression. *EMBO J.* **1995**, *14* (18), 4514−4522.
(98) Zwicker, J.; Gross, C.; Lucibello, F. C.; Truss, M.; Ehiert, F.; Engeland, K.; Müller, R. Cell Cycle Regulation of cdc25C Transcription Is Mediated by the Periodic Repression of the Glutamine-Rich Activators NF-Y and Sp1. *Nucleic Acids Res.* **1995**, *23* (19), 3822−3830.

(99) de Sousa Abreu, R.; Penalva, L. O.; Marcotte, E. M.; Vogel, C. Global Signatures of Protein and mRNA Expression Levels. *Mol. BioSyst.* **2009**, *5* (12), 1512−1526.
(100) Liu, Y.; Beyer, A.; Aebersold, R. On the Dependency of Cellular Protein Levels on mRNA Abundance. *Cell* **2016**, *165* (3), 535−550.
(101) Azami, S.; Wagatsuma, A.; Sadamoto, H.; Hatakeyama, D.; Usami, T.; Fujie, M.; Koyanagi, R.; Azumi, K.; Fujito, Y.; Lukowiak, K.; Ito, E. Altered Gene Activity Correlated with Long-Term Memory Formation of Conditioned Taste Aversion inLymnaea. *J. Neurosci. Res.* **2006**, *84* (7), 1610−1620.
(102) Lu, T. Z.; Feng, Z.-P. A Sodium Leak Current Regulates Pacemaker Activity of Adult Central Pattern Generator Neurons in Lymnaea Stagnalis. *PLoS One* **2011**, *6* (4), No. e18745.
(103) Korneev, S. A.; Kemenes, I.; Straub, V.; Staras, K.; Korneeva, E. I.; Kemenes, G.; Benjamin, P. R.; O'Shea, M. Suppression of Nitric Oxide (NO)-Dependent Behavior by Double-Stranded RNA-Mediated Silencing of a Neuronal NO Synthase Gene. *J. Neurosci.* **2002**, *22* (11), No. RC227.
(104) Abe, M.; Kuroda, R. The Development of CRISPR for a Mollusc Establishes the Formin Lsdia1 as the Long-Sought Gene for Snail Dextral/Sinistral Coiling. *Development* **2019**, *146* (9), No. dev175976.
(105) Scheibenstock, A.; Krygier, D.; Haque, Z.; Syed, N.; Lukowiak, K. The Soma of RPeD1Must Be Present for Long-Term Memory Formation of Associative Learning in Lymnaea. *J. Neurophysiol.* **2002**, *88* (4), 1584−1591.
(106) Spencer, G. E.; Syed, N. I.; Lukowiak, K. Neural Changes after Operant Conditioning of the Aerial Respiratory Behavior in Lymnaea Stagnalis. *J. Neurosci.* **1999**, *19* (5), 1836−1843.
(107) Syed, N. I.; Winlow, W. Respiratory Behavior in the Pond Snail Lymnaea Stagnalis: II. Neural Elements of the Central Pattern Generator (CPG). *J. Comp. Physiol., A* **1991**, *169* (5), 557−568.
(108) Neveu, C. L.; Huan, Y.; Momohara, Y.; Patel, P. R.; Chiel, H. J.; Chestek, C. A.; Byrne, J. H. Combining Voltage-Sensitive Dye, Carbon Fiber Array, and Extracellular Nerve Electrodes Using a 3-D Printed Recording Chamber and Manipulators. *J. Neurosci. Methods* **2023**, *396*, No. 109935.
(109) Costa, R. M.; Baxter, D. A.; Byrne, J. H. Neuronal Population Activity Dynamics Reveal a Low-Dimensional Signature of Operant Learning in Aplysia. *Commun. Biol.* **2022**, *5* (1), No. 90.
(110) Zilionis, R.; Nainys, J.; Veres, A.; Savova, V.; Zemmour, D.; Klein, A. M.; Mazutis, L. Single-Cell Barcoding and Sequencing Using Droplet Microfluidics. *Nat. Protoc.* **2017**, *12* (1), 44−73.
(111) Yang, L.; George, J.; Wang, J. Deep Profiling of Cellular Heterogeneity by Emerging Single-Cell Proteomic Technologies. *Proteomics* **2020**, *20* (13), No. 1900226.
(112) Wattenberg, B. W. Kicking off Sphingolipid Biosynthesis: Structures of the Serine Palmitoyltransferase Complex. *Nat. Struct. Mol. Biol.* **2021**, *28* (3), 229−231.
(113) Kalinichenko, L. S.; Gulbins, E.; Kornhuber, J.; Müller, C. P. Sphingolipid Control of Cognitive Functions in Health and Disease. *Prog. Lipid Res.* **2022**, *86*, No. 101162, DOI: 10.1016/j.plipres.2022.101162.

https://doi.org/10.1021/acs.jproteome.4c00055
J. Proteome Res. 2025, 24, 27−45